

**ENGINEERING REPORTER TAGS IN FLAVIVIRUSES
TO PROBE VIRAL STRUCTURE AND MORPHOGENESIS**

by

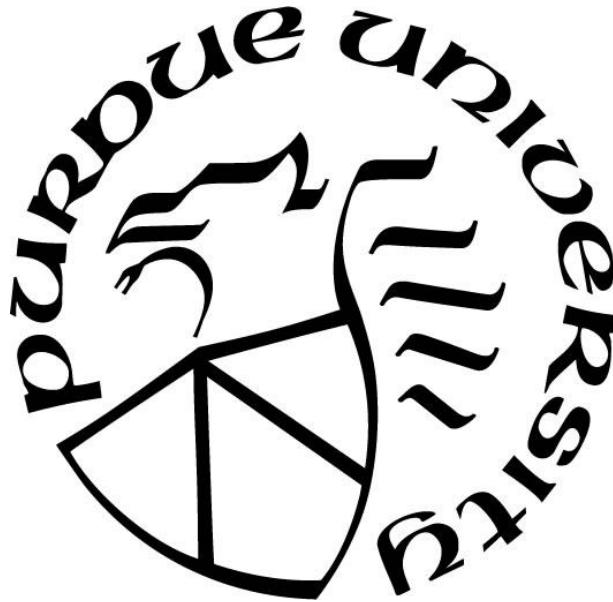
Matthew Lerdahl

A Thesis

Submitted to the Faculty of Purdue University

In Partial Fulfillment of the Requirements for the degree of

Master of Science



Department of Biological Sciences

West Lafayette, Indiana

May 2020

**THE PURDUE UNIVERSITY GRADUATE SCHOOL
STATEMENT OF COMMITTEE APPROVAL**

Dr. Richard J. Kuhn, Chair

School of Biological Sciences

Dr. Douglas LaCount

School of Medicinal Chemistry and Molecular Pharmacology

Dr. Cynthia Stauffacher

School of Biological Sciences

Approved by:

Dr. Janice Evans

The views expressed in this thesis are those of the author and do not reflect the official policy or position of the United States Air Force, Department of Defense, or the U.S. Government

ACKNOWLEDGMENTS

There are many people I would like to thank but most importantly my advisor, Dr. Richard Kuhn. After graduating from the Air Force Academy, I had very little/no experience in virology. Dr. Kuhn still welcomed me into his lab, and, because of his guidance, I've learned more during my time at Purdue than I ever thought possible. Without his direction and expertise, I would never have become the scientist and critical thinker that I am today.

I would also like to thank my committee members, Dr. Cynthia Stauffacher and Dr. Douglas LaCount, who were always willing to help and provide excellent constructive criticism that bettered my project. Their thoughtful suggestions and questions prompted me to more deeply investigate aspects of my research that I may otherwise not have.

Next, I would like to thank my fellow lab mates for always being there for me. Specifically, Thu Cao, Conrad Nicholls, Andrew Miller, and Carlos Brito who answered my many questions and were great role models for an aspiring scientist and researcher like myself. Importantly, I would like to sincerely thank my mentor Dr. Devika Sirohi. Without her constant help and support, none of this research would have been possible. She taught me everything I needed to know about virus research and did so with kindness, patience, and tact. Furthermore, she helped me with the planning and execution of many of the experiments described in this thesis and for that, I am sincerely grateful. I also want to thank Anita Robinson for all her help with scheduling and administrative details which made my time here much easier.

A big thanks to the Purdue Military Research Institute for providing funding and coordinating a smooth transition from the Air Force Academy to Purdue. PMRI is a great program that will no doubt benefit all branches of the military for years to come.

Finally, I want to thank my wonderful family and friends for keeping me sane throughout my time at Purdue. Specifically, my mom and girlfriend for their unwavering support and encouragement.

TABLE OF CONTENTS

LIST OF TABLES	8
LIST OF FIGURES	9
LIST OF ABBREVIATIONS.....	10
ABSTRACT.....	12
CHAPTER 1. INTRODUCTION	14
1.1 Flaviviridae	14
1.2 Overview of select members.....	14
1.2.1 Dengue virus.....	14
1.2.2 Hepatitis C virus	15
1.3 Flaviviridae life cycle	16
1.3.1 Flavivirus life cycle	16
1.3.2 Hepacivirus life cycle	18
1.4 Flavivirus genome and proteins	20
1.4.1 Envelope protein	21
1.4.2 Capsid protein.....	22
1.4.3 Pre-membrane/Membrane protein.....	22
1.4.4 Nonstructural proteins	22
1.5 Hepacivirus genome and proteins.....	23
1.5.1 Envelope-1/Envelope-2 proteins	24
1.5.2 Core protein	25
1.5.3 Nonstructural proteins	25
1.6 Protein and epitope tags	26
1.6.1 Luminescent tags	26
1.6.2 Affinity tags.....	27
1.6.3 HiBiT reporter system	29
CHAPTER 2. GENERATION AND CHARACTERIZATION OF REPORTER FLAVIVIRUSES	30
2.1 Chapter Summary	30
2.2 Introduction.....	30

2.3	Materials and methods	32
2.3.1	Cell culture.....	32
2.3.2	Site-directed mutagenesis	32
2.3.3	In vitro transcription and transfection of vRNA.....	32
2.3.4	HiBiT assay	33
2.3.5	Plaque assay.....	33
2.3.6	Infections	33
2.3.7	Density gradient centrifugation	33
2.3.8	SDS-PAGE and western blot.....	34
2.4	Results.....	34
2.4.1	Development of HiBiT methodology and replication of previous findings	34
2.4.2	Determination of suitable HiBiT loci and construct variation.....	36
2.4.3	Characterization of recombinant DENV replication and translation competence.....	39
2.4.4	Characterization of recombinant DENV infectious particle production	41
2.4.5	C-103 HiBiT signal is associated with the DENV particle	46
2.4.6	Composition of insert within E protein is critical for infectious particle production	48
2.5	Discussion.....	50
CHAPTER 3. GENERATION AND CHARACTERIZATION OF REPORTER HEPACIVIRUSES		54
3.1	Chapter Summary	54
3.2	Introduction.....	54
3.3	Materials and Methods.....	56
3.3.1	Cell culture.....	56
3.3.2	Site directed mutagenesis	56
3.3.3	In vitro transcription and transfection of vRNA.....	57
3.3.4	HiBiT assay	57
3.3.5	Focus unit identification assay.....	57
3.3.6	Immunofluorescence assay.....	58
3.3.7	SDS-PAGE and western blot.....	58
3.3.8	FLAG affinity purification	58
3.4	Results.....	59

3.4.1	Determination of insert loci and construct variation	59
3.4.2	Initial characterization of recombinant HCV replication and translation.....	60
3.4.3	Characterization of recombinant HCV infectivity.....	62
3.4.4	FLAG Immunoprecipitation	65
3.5	Discussion.....	66
CHAPTER 4. CONCLUSIONS AND FUTURE DIRECTIONS.....		69
REFERENCES		74

LIST OF TABLES

Table 2.1. DENV-HiBiT tag location and construct variation.....	37
Table 3.1. HCV-HiBiT tag locations and construct variation.....	60

LIST OF FIGURES

Figure 1.1. Flavivirus life cycle.....	17
Figure 1.2. Hepacivirus life cycle.....	19
Figure 1.3. Flavivirus polyprotein processing	20
Figure 2.1. Evaluation of HiBiT recombinant DENV NS1 tag sites	36
Figure 2.2. HiBiT loci position in genome and mature E-M structure.....	38
Figure 2.3. Luminescence of electroporated cells at 48 hours.....	41
Figure 2.4. Luminescence of infected cells at 72 hours post infection.....	43
Figure 2.5. Infectious titer of recombinant clones following electroporation.....	44
Figure 2.6. Infectious titer and HiBiT activity of C-103.....	45
Figure 2.7. Infectious titer and HiBiT activity of M-55.....	46
Figure 2.8. HiBiT activity and infectious titer for each fraction following density gradient fractionation.....	47
Figure 2.9. Infectious titer of recombinant virus containing FLAG and SmBiT epitopes.....	49
Figure 3.1. Insert loci and composition within HCV genome.....	60
Figure 3.2. Luminescence of transfected cells at 24 to 96 hours post transfection.....	61
Figure 3.3. Infectivity of recombinant virus assessed by immunofluorescence.....	63
Figure 3.4. Peak titer and HiBiT activity for recombinant HCV.....	65
Figure 3.5. FLAG immunoprecipitation with efficiency determined by HiBiT activity.....	66

LIST OF ABBREVIATIONS

Å	Angstrom
ADE	Antibody dependent enhancement
apoE	Apolipoprotein E
BHK	Baby hamster kidney
BiT	Binary technology
bNAbs	Broadly neutralizing antibodies
BSA	Bovine serum albumin
C	Capsid protein
cDNA	Complementary deoxyribonucleic acid
CO ₂	Carbon dioxide
CPE	Cytopathic effect
Cryo-EM	Cryo-electron microscopy
Cryo-ET	Cryo-electron tomography
DENV	Dengue virus
DHF	Dengue hemorrhagic fever
DMEM	Dulbecco's modified eagle media
DSS	Dengue shock syndrome
E	Envelope protein
ER	Endoplasmic reticulum
Fab	Antigen binding fragment
FBS	Fetal bovine serum
FFU	Focus forming unit
GFP	Green fluorescent protein
HCV	Hepatitis C virus
HDL	High-density lipoprotein
HIS	Polyhistidine tag
HPSG	Heparan sulfate proteoglycans
IRES	Internal ribosomal entry site
JEV	Japanese encephalitis virus

kb	Kilobases
kDa	Kilodalton
LgBiT	Large BiT
LVP	Lipoviral particle
M	Membrane protein
MEM	Minimum essential media
miRNA	MicroRNA
MOI	Multiplicity of infection
nm	Nanometers
NMR	Nuclear magnetic resonance
NS	Nonstructural
ORF	Open reading frame
PBS	Phospho-buffered saline
PCR	Polymerase chain reaction
PFU	Plaque forming unit
PI	Propidium iodide
prM	Pre-membrane protein
RdRp	RNA dependent RNA polymerase
RLU	Relative light unit
SDM	Site-directed mutagenesis
SmBiT	Small BiT
STREP	Streptavidin tag
SVP	Subviral particle
TGN	Trans-golgi network
UTR	Untranslated region
VLDL	Very low-density lipoprotein
VLP	Virus-like particle
vRNA	Viral ribonucleic acid
WNV	West Nile virus
ZIKV	Zika virus

ABSTRACT

The family *Flaviviridae* includes important genera such as flavivirus and hepacivirus which comprise significant human pathogens that affect hundreds of millions annually. The understanding of these viruses, the viral life cycle, and pathogenicity is vital when it comes to developing therapeutics. Flavivirus virions undergo major conformational rearrangements during the life cycle, including the assembly and maturation steps. In order to create a reagent to investigate these processes, luminescent reporter viruses have been constructed. Luminescent reporter tags have yet to be incorporated into the structural proteins of dengue virus (DENV) without significantly affecting replication or infectivity and successful tagging would allow for targeted studies examining access to specific structural epitopes. Engineering tags in DENV structural proteins is particularly difficult because most reporter tags involve large insertions which may create steric hindrance and inhibit proper protein folding. However, the reporter system described here, developed by Promega, is much smaller than a full-size luciferase protein. It involves an eleven amino acid subunit (HiBiT) tagged to a viral protein that creates measurable luminescence when incubated with the larger subunit (LgBiT). Using the structure of the virion as a guide, the HiBiT reporter tag was incorporated into the structural region of the DENV genome including sites in capsid (C) as well as the glycoproteins membrane (M) and envelope (E). Resulting recombinant viruses were characterized and tag sites within the C protein membrane anchor as well as the transmembrane domain of M protein were found to tolerate HiBiT insertion and produce infectious particles. The recombinant virus possessing HiBiT in C protein was found to be stable over three rounds of serial passaging while virus containing the M protein tag site was found to be unstable. HiBiT activity of the capsid tagged virus was also found to directly correlate with purified infectious particles, suggesting the capsid membrane anchor may remain associated with the virus even after polyprotein processing. Additionally, insert composition was found to be a key determinant for the production of infectious virus. The lessons learned from engineering HiBiT in the DENV system were then applied to hepatitis C virus (HCV).

The highly lipophilic and pleiomorphic nature of HCV has made structural studies particularly difficult. However, by constructing multi-tagged reporter viruses containing both HiBiT and various purification tags, researchers will save time and resources in preparation for structural studies which are vital for vaccine development. In this study, HiBiT was incorporated

into sites within HCV previously shown to tolerate tags of various sizes. Different insert compositions were engineered within the genome and the construct containing both FLAG and HiBiT tags within the N-terminus of E2 yielded highly infectious and quantifiable, luminescent virus. The recombinant HCV containing FLAG and HiBiT displayed similar peak titer as compared to WT while also demonstrating HiBiT activity. Furthermore, the FLAG peptide was found to be partially surface exposed and capable of being used for virus purification purposes. The multi-tagged reporter virus characterized in this study provides a robust platform for quantification and purification of HCV, two facets of research that are critical for the determination of viral structure via cryo-EM and other imaging techniques. The findings from both the DENV and HCV studies provide a robust foundation for future tagging of viruses within the family *Flaviviridae* and offer insight on the structural proteins that compose the virion.

CHAPTER 1. INTRODUCTION

1.1 Flaviviridae

Flaviviruses, family *Flaviviridae*, impact hundreds of millions of people each year resulting in high rates of morbidity and mortality worldwide. Within the genus there are several significant human pathogens such as dengue virus (DENV), Zika virus (ZIKV), and West Nile virus (WNV), among many others. Also included in the family *Flaviviridae* is the hepacivirus genus consisting of Hepatitis C virus (HCV), a bloodborne pathogen responsible for a tremendous public health burden (WHO, 2019). Flavivirus infection is one of the leading causes of disease in humans with symptoms ranging anywhere from slight rash and joint pain to hemorrhagic fever. Reported infections are mostly concentrated in tropical and subtropical regions due to their transmission via arthropod vectors such as *Aedes aegypti*. As the habitat for these arthropod vectors increases, so too does the infection rate within previously unaffected areas (Morales et al., 2017). Due to the growing infection rate and global health concern, a comprehensive understanding of flavivirus life cycle and pathogenicity is more important than ever.

1.2 Overview of select members

1.2.1 Dengue virus

DENV has four serotypes which account for an estimated 390 million infections each year; of which, anywhere from 67 to 136 million manifest clinically (WHO, 2019). Additionally, several studies indicate a continued increase in global incidence over the past few decades and estimate that over 3.9 billion people are now at risk of infection with DENV (Brady et al., 2012). A majority of DENV infections are asymptomatic or subclinical, but some infections result in severe flu-like symptoms. Although not as prevalent, DENV infection may progress to dengue hemorrhagic fever (DHF) and dengue shock syndrome (DSS), which involve severe bleeding, organ impairment, and/or plasma leakage (WHO, 2019).

Infection, and subsequent recovery, from one DENV will provide lifelong immunity against that particular serotype. However, any cross-immunity to other serotypes will subside. Subsequent infections with a different serotype may increase the severity of disease and the risk

of developing DHF/DSS (WHO, 2019). Currently, there are no specific treatments for dengue fever. Advanced medical care from trained professionals has resulted in decreased mortality rates from ~20% to less than 1%, but, in some lesser developed regions, the mortality rates remain high (Rajapakse et al., 2011). There are several vaccines currently in clinical trials and one commercially available under the brand name Dengvaxia. However, these vaccines face many challenges including antibody dependent enhancement (ADE), a phenomenon in which the antibodies bind to surface proteins but do not inactivate the virus, increasing the likelihood of developing severe dengue (Flipse et al., 2016). In order to overcome these challenges, researchers must be armed with insights into the viral envelope, protein conformations, and the DENV particle structure (Mukhopadhyay et al., 2005).

1.2.2 Hepatitis C virus

HCV, the lone species in the hepacivirus genus, is one of the leading causes of cirrhosis, hepatocellular carcinoma, and liver-related deaths in humans (Milliman et al., 2017). The virus can lead to both acute and chronic hepatitis with severity depending on a number of virologic and host genetic factors. Approximately 30% of those infected will spontaneously clear the virus through a multitude of immunological factors within 6 months without the need for treatment. The remaining 70% will likely develop chronic HCV infection. The symptoms of HCV infection range anywhere from mild illness to serious, lifelong conditions like those stated above. An estimated 71 million people have chronic HCV infection globally and a large proportion of those individuals will likely develop cirrhosis or liver cancer (WHO, 2019). Unlike flaviviruses, HCV is a bloodborne pathogen with the most common modes of infection and transmission being injection drug use, unsafe injection practices, or sexual practices which lead to exposure of blood (WHO, 2019). Additionally, HCV is highly infectious and exposure to a small amount of virus particles can lead to infection (Pfaender et al., 2018).

Despite the seriousness of long-term, chronic infection, more than 95% of affected individuals can be cured with antiviral medication. However, access to diagnosis and treatment is low. The average total cost of a 12-week course of antivirals in the US is around \$84,000 with additional combinatorial approaches costing much more (Henry, 2018). Furthermore, there is currently no effective vaccine for HCV. In order to produce more accessible medication and develop a useful vaccine, researchers must first understand the structural and immunological

mechanisms of infection clearance. Currently, there is ongoing research involving the structural analysis of broadly neutralizing antibodies (bNAbs) which may reveal key details about the underlying mechanisms of infection clearance and, ultimately, lead to a vaccine. However, the proper tools to enable high resolution structural analysis would likely be necessary to achieve this goal (Kinchen et al., 2018).

1.3 Flaviviridae life cycle

1.3.1 Flavivirus life cycle

Flaviviruses, a genus containing more than 70 different viruses, all follow a similar process of entry, replication, and virus release. Entry is first initiated upon direct contact of the envelope glycoprotein (E) with one or more hypothesized host receptors such as C-type lectin CD209 antigen (DC-SIGN) (Figure 1.1) (Mukhopadhyay et al., 2005). Binding triggers receptor-mediated endocytosis which involves clathrin pits forming in the host cell membrane. Once in the endosome, the acidic environment causes an irreversible trimerization of E protein which results in fusion of viral and endosomal membrane. Particle disassembly occurs and the viral genome is released into the cytoplasm. Once in the cytoplasm, the positive sense viral RNA (vRNA) is translated into a single polyprotein. Viral and host proteases process the polyprotein both co- and post-translationally. The viral proteins are transported to the endoplasmic reticulum (ER) where the nonstructural proteins aid in forming ER-derived vesicle packets which serve as the site of genome replication (Gillepsie et al., 2010). Virus assembly occurs on the surface of the ER. Newly synthesized capsid proteins (C) associate with vRNA to nucleate assembly and bud through the ER membrane (Li et al., 2008). During this portion of the life cycle, the viral particle is in its immature state, which consists of 60 trimeric, spike-like projections of E protein and pre-membrane protein (prM). This conformation is formed in order to prevent premature membrane fusion due to the prM protein occluding the fusion loop on E protein (Yu et al., 2009). The immature particles are transported through the trans-Golgi network (TGN) where the host-protease furin cleaves prM. The pr peptide remains associated with the viral particle until released into the neutral pH environment of the extracellular milieu (Yu et al., 2009). Mature particles are subsequently released via exocytosis and ready to infect naïve host cells.

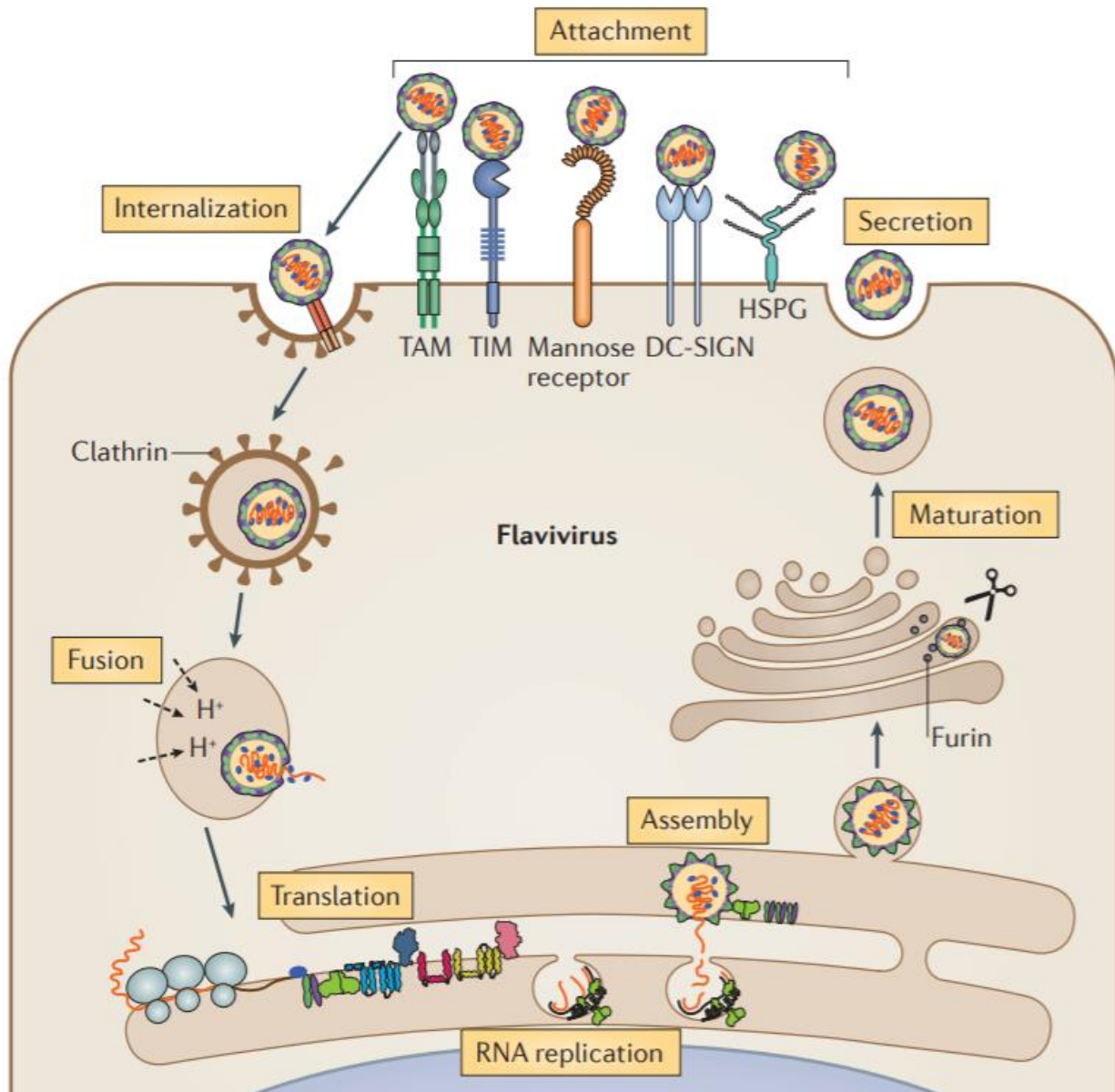


Figure 1.1. Flavivirus life cycle. Flaviviruses follow a sequential progression upon attachment to the host cell. The particles enter the cell via clathrin-dependent, receptor-mediated endocytosis. An acidic pH in the late endosome triggers conformational changes which allow fusion and the release of genomic material. The positive sense RNA is recognized by ribosomes, translated in the ER, and a polyprotein is produced. Host and viral proteases co- and post-translationally process the polyprotein and the nonstructural proteins form the replication complex for the synthesis of new proteins. The nucleocapsid nucleates a new virus particle and buds from the ER membrane and enters the secretory pathway. In the TGN, the pr peptide is cleaved by furin but remains attached to the particle until secretion. Used with permission from *Nature Reviews Microbiology* and Neufeldt et al. (Neufeldt et al., 2018).

1.3.2 Hepacivirus life cycle

The hepacivirus life cycle is similar to flaviviruses but with a few important differences. The virus particle targets hepatocytes and is transported to the surface of the cell via the bloodstream. The particle is enveloped with a lipid membrane that the glycoproteins, envelope 1 and envelope 2 (E1 and E2), are anchored to. These proteins are hypothesized to play a role in entry, or at least cell attachment, where apolipoprotein E (apoE) and cell surface heparan sulfate proteoglycans (HPSG), among other surface receptors, interact (Figure 1.2) (Alazard-Dany et al., 2019). Binding to these receptors can cause downstream signaling which promotes the lateral movement of the particle to sites of cell-cell contact. HCV then enters via the endocytic pathway and fuses with the membrane based on endosomal acidification. Like flaviviruses, the viral RNA is translated as a single polyprotein which is co- and post-translationally processed by both host and viral proteases. In the case of HCV, there are liver-specific microRNA (miRNA), such as miR-122, which are essential for replication and translation. Viral assembly of HCV is still poorly understood but occurs near replication complexes at assembly sites associated with ER-derived membranes (Miyazari et al., 2007). Viral nonstructural (NS) protein 2 and p7 also play a key role by facilitating the recruitment of core protein (core) and E1-E2 to assembly sites (Alazard-Dany et al., 2019). Although the exact mechanisms of maturation are not entirely understood, as the HCV particle moves through the secretory pathway, glycan modification, as well as possible rearrangement of E1-E2 disulfide bonds, may occur (Lindenbach et al., 2013). HCV particles also interact with lipoproteins throughout the secretory pathway, and certain cell lines, such as Huh-7 cells, can produce very-low-density-lipoprotein (VLDL) particles which are under-lipidated. HCV particles can have a wide range of densities and lipid compositions which can make the quantification and purification of virus difficult (Miyazari et al., 2007). During maturation, p7 also acts as a viroporin which equilibrates pH gradients and stabilizes particles on the way to excretion. HCV particles acquire their low buoyant density via interactions with apoE-containing VLDLs or high-density lipoproteins (HDL). Virus particles are excreted via the secretory pathway and are protected by p7 from low pH exposure which would otherwise neutralize intracellular compartments (Wozniak et al., 2010).

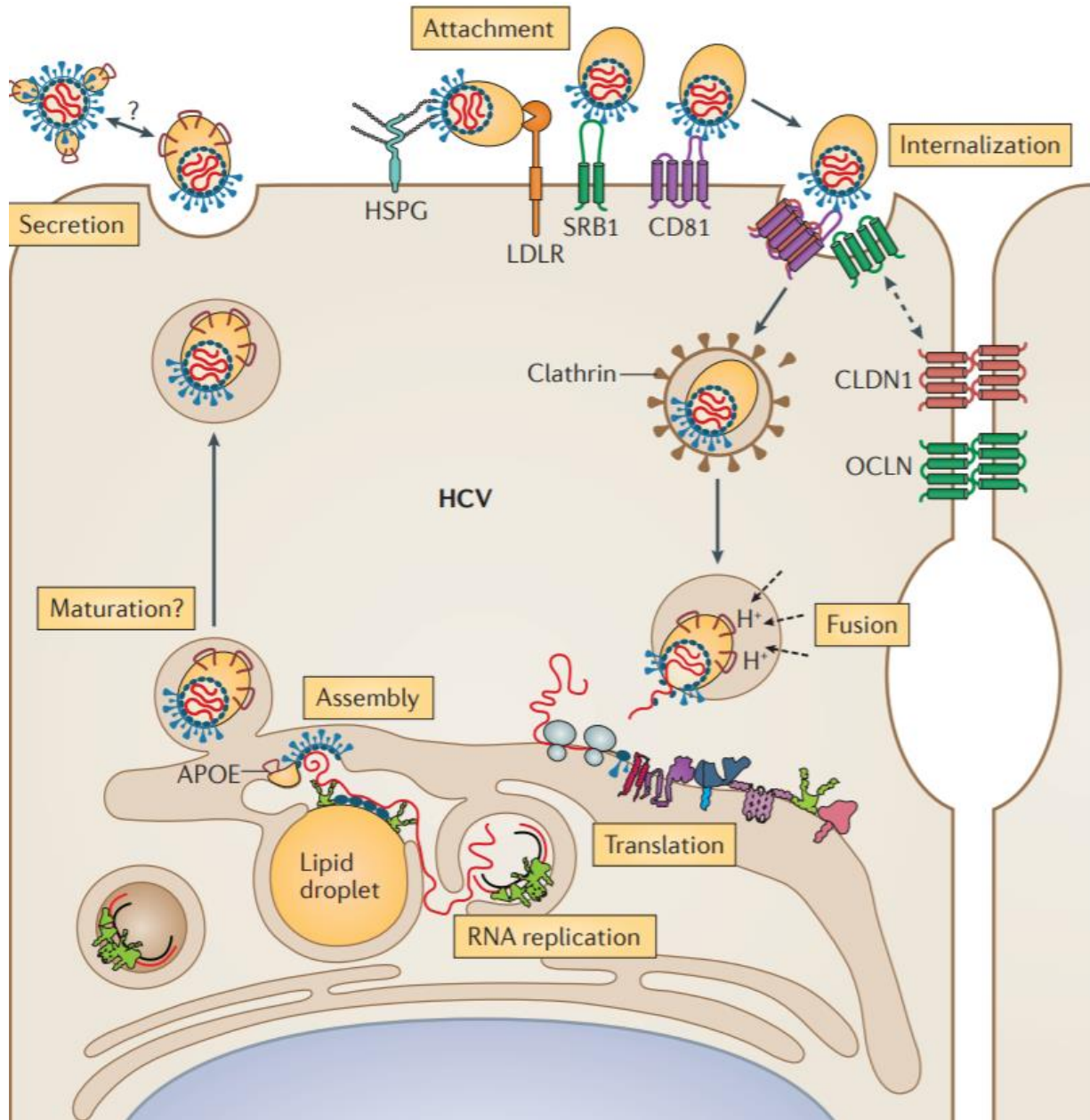


Figure 1.2. Hepacivirus life cycle. HCV particles bind to receptors such as HSPG and low-density-lipoprotein receptors and laterally diffuse towards the apical membrane. They then enter via clathrin-dependent, receptor-mediated endocytosis. Genomic material is released into the cytosol and translated at the ER where host cell factors and viral proteins form the replication complex. Particle assembly occurs with cytosolic lipid droplets at sites enriched with core protein, envelope glycoproteins, p7, and NS2. Formation and secretion of virions occurs in association with VLDL machinery. The acquisition of apoE aids in the maturation of the particle and possibly particle release. HCV can also form lipovirions or bind to VLDL particles after release. Used with permission from *Nature Reviews Microbiology* and Neufeldt et al. (Neufeldt et al., 2018).

1.4 Flavivirus genome and proteins

Flaviviruses are enveloped positive-sense single stranded RNA viruses with a genome of approximately 11 kilobases (kb) (Mukhopadhyay et al., 2005). The particle is about 50 nanometers (nm) in diameter and contains capsid proteins with a capped RNA genome at its core. Surrounding the capsid proteins is a host-derived lipid membrane serving as the virus envelope with embedded membrane and glycoproteins. E protein arranges in a quasisymmetric T=3 array which consists of 90 homodimers forming a smooth surface interface following maturation (Kuhn et al., 2002). Prior to maturation, E and prM/M proteins form 60 trimeric, spike-like projections which prevent immature fusion.

The flavivirus genome is translated using a single open reading frame (ORF) which results in a large polyprotein (Figure 1.3). Following translation, the polyprotein is processed by both cellular and viral proteases producing 10 proteins that each play a role in the viral life cycle. The 3 structural proteins (C, prM, and E) are used to build new virus particles while the 7 nonstructural proteins (NS1, 2A, 2B, 3, 4A, 4B, and 5) primarily function as replication proteins (Mukhopadhyay et al., 2005).

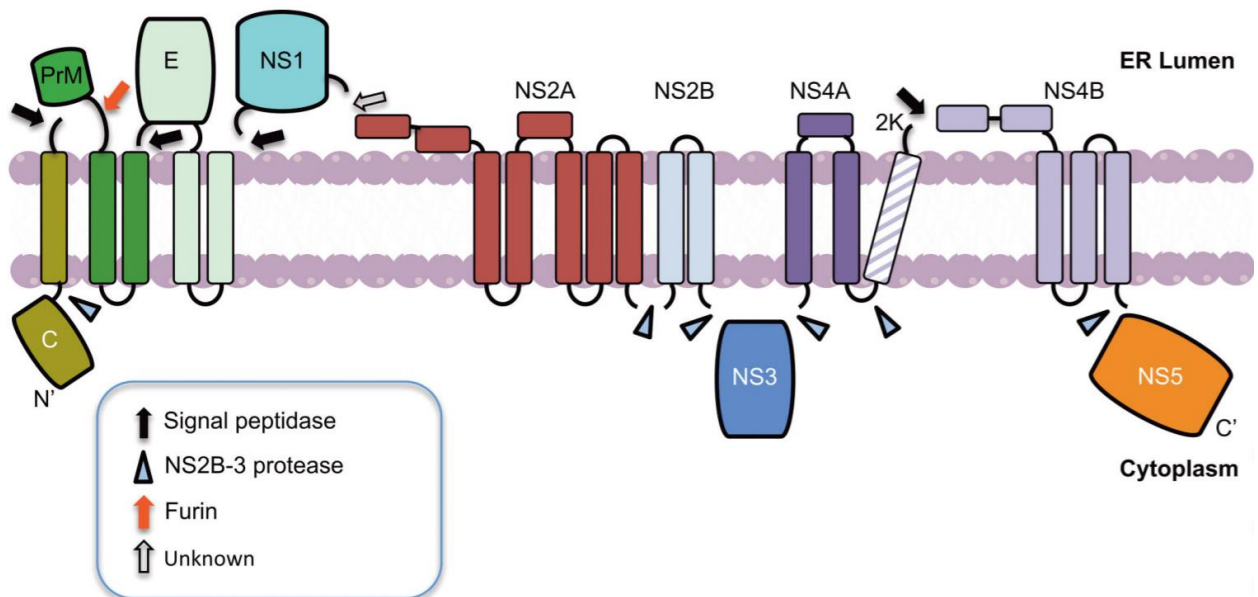


Figure 1.3. Flavivirus polyprotein processing. Following translation of the viral polyprotein, host and viral proteases cleave at the indicated junctions. ER membrane is shown in pink and transmembrane domains are connected by loops depicted as lines. Black, blue, and red arrows represent signal peptidase, NS2B-3 protease, and furin protease cleavage sites, respectively. Used with permission from *Current Opinion in Virology* and Apte-Sengupta et al. (Apte-Sengupta et al., 2014).

1.4.1 Envelope protein

E protein, a structural protein in flaviviruses, plays an important role in viral infections. In the mature particle, the E glycoproteins are arranged in 90 homodimers which lay flat in a herringbone pattern along the particle surface. E protein is approximately 53-60 kilodaltons (kDa) and each monomer is composed of three β -barrels which are divided into three different structural domains: EDI, EDII, and EDIII in addition to the stem-anchor region. The structure for the ectodomain of E protein has been determined by X-ray crystallography, nuclear magnetic resonance (NMR) spectroscopy, and electron cryo-microscopy (cryo-EM) with some structures as low as 3.1 Angstrom (\AA) resolution (Sevanna et al., 2018). Structural and functional studies have revealed that each of the domains serve distinct and vital roles in the flavivirus life cycle (Zhang et al., 2017).

EDI contains ~120 residues which form an eight-stranded β -barrel. It is thought to stabilize the overall orientation of E protein and has a conserved N-linked glycosylation site at residue Asn 154. However, in DENV, glycosylation occurs at Asn 67 and Asn 153 (Wen et al., 2018). Recent studies have also demonstrated that EDI may play a role in pH sensitivity and neuroinvasiveness (Beasley et al., 2005). EDI and EDII are connected via discontinuous peptides to form the hinge region, which contains a ligand binding pocket (Zhang et al., 2017). EDII contains the fusion peptide which allows for virus-mediated membrane fusion. The low pH within the late endosome triggers a conformational change exposing the fusion loop and results in fusion and the release of genomic material (Fritz et al., 2011). EDII is also responsible for facilitating E homodimerization and mutations in this region can reduce virulence (Yu et al., 2013). EDIII is a globular domain that resides opposite of EDI. Composed of ~100 amino acids (aa), it is believed to participate in receptor recognition and contain important linear antigenic epitopes that interact with neutralizing antibodies (Matsui et al., 2010). Mutations in this region have been demonstrated to drastically affect host cell tropism and virulence and many of the neutralizing antibody binding epitopes are conserved across viruses meaning they could potentially be used as a therapeutic target (Kanai et al., 2006, Sun et al., 2018).

1.4.2 Capsid protein

C protein is the first protein encoded in the flavivirus genome and is proteolytically processed at the N- and C- termini of the transmembrane anchor junctions (Figure 3) (Stocks et al., 1998). At approximately 12 kDa in size, C protein can exist both as a membrane-associated protein as well as a free monomer which can form homodimers in solution. The protein is highly basic with an affinity for both nucleic acids and lipid membranes and, thus, is proposed to nucleate assembly (Jones et al., 2003). It has been demonstrated that C protein assists in nucleic acid arrangements and can act as an RNA chaperone *in vitro* and winds the vRNA into the particle to form the nucleocapsid. Although the C protein structure within the virus particle is not yet fully resolved to subatomic resolution, structural studies have shown residual density fitting the approximate size of C protein near the particle surface; which may indicate C protein interactions with the transmembrane portions of E and M proteins during the immature state of the virus (Therkelsen et al., 2018). This notion is further supported by cryo-EM studies revealing helix $\alpha 5$ of C protein being inserted into the viral membrane (Tan et al., 2020).

1.4.3 Pre-membrane/Membrane protein

The prM protein is the precursor to M protein and initially forms a heterodimer with E protein in the immature state of the virus particle. Upon exposure to the acidic environment of the TGN, prM is proteolytically cleaved by host protease furin which converts the spiky, immature particle into a smooth, infectious virus. However, the pr peptide remains attached to the particle (in order to prevent premature fusion) until it is released into the extracellular milieu and exposed to a more neutral pH (Sirohi et al., 2016). M protein is an 8 kDa fragment of its precursor form, prM, and is anchored to the membrane via two transmembrane helices. In the mature particle, M forms homodimers with E protein.

1.4.4 Nonstructural proteins

The nonstructural proteins of flaviviruses consist of NS1, 2A, 2B, 3, 4A, 4B, and 5, each of which play important and distinct roles in the replication and assembly of flaviviruses. NS1 is a highly conserved protein amongst flaviviruses and the intracellular dimer plays a role in genome replication whereas the secreted hexamer plays a role in immune evasion (Rastogi et al., 2016).

Intracellular NS1 is targeted to the ER and forms a replication complex constructed from ER derived vesicle packets. The secreted form of NS1 serves as a diagnostic marker for detection of infection but has also been shown to affect signal transduction pathways and can modulate the pathogenesis of certain flaviviruses (Rastogi et al., 2016).

Two hydrophobic proteins, NS2A and B, are encoded upstream of NS3. NS2B serves as the protease cofactor of NS3 while NS2A is an essential component of the replicase (Khromykh et al., 2000). NS2A has been shown to play a vital role in the incorporation of genomic RNA into the budding virion and interacts with other nonstructural proteins to aide in virus assembly (Murray et al., 2008). NS3 performs a variety of different functions throughout the viral life cycle including: forming a serine protease which is responsible for cleavage of the viral polyprotein, helicase activity, and even inducing apoptosis through caspase interactions (Amberg et al., 1994, Patkar et al., 2008). NS4A/B are important for membrane rearrangement which leads to replication complex formation. Cleavage regulation, facilitated by a transmembrane 2K peptide, allows for interaction of NS4A/B with other nonstructural proteins like NS1 and NS3 (Shiryayev et al., 2010). Additionally, NS4B is thought to play a role in immune evasion and is deeply involved with the host immune response (Kelley et al., 2011). NS5 is the largest of the flavivirus proteins and possesses RNA-dependent RNA polymerase (RdRp), methyltransferase, and guanylyltransferase activities (Murray et al., 2008).

1.5 Hepacivirus genome and proteins

Like all *Flaviviridae*, hepaciviruses are enveloped positive-sense single stranded RNA viruses. The HCV genome is approximately 9 kb and the virus particles range in size anywhere from 40 to 100 nm in diameter (Catanese et al., 2013). The non-capped RNA is contained within the core protein, and the ORF codes for 11 different proteins with a 341 nucleotide (nt) 5' untranslated region (UTR) containing an internal ribosomal entry site (IRES) which can form a stable, translation pre-initiation complex (Jubin et al., 2000). The structural proteins include core, E1, and E2, while the nonstructural proteins include p7, NS2, NS3, NS4A, NS4B, NS5A, and NS5B. HCV is the most structurally pleiomorphic member of the *Flaviviridae* family with particles forming spherical, spike-like projections of E1 and E2 heterodimers (Catanese et al., 2013).

1.5.1 Envelope-1/Envelope-2 proteins

E1 and E2 are the two envelope glycoproteins which compose the HCV virion envelope and play vital roles in entry and fusion. Both E1 and E2 are type I transmembrane glycoproteins with ectodomains of 160 and 354 aa, respectively, and a C-terminal transmembrane domain of approximately 30 aa (Chevaliez et al., 2006). The structure of the envelope proteins has yet to be solved at a high enough resolution to enable advanced structural/antibody binding studies. However, some 3D-structural information has been elucidated from cryo-EM and cryoelectron tomography (cryo-ET). One such finding revealed that HCV particles incorporate apoB and apoA-I in addition to apo-E (Catanese et al., 2013). Further structural studies have been able to classify some antibody binding patterns and show that some mechanisms of bNAb mediated clearance is dependent on binding primarily to E2, with additional binding profiles showing partial binding to E1 (Kinchen et al., 2018).

Similar to flaviviruses, the envelope proteins have a variety of functions including ER localization, dimer assembly, and membrane anchoring. The conformations of E1 and E2 are interdependent and, therefore, functional studies of the envelope proteins tend to treat the two as a complex (Kong et al., 2013). Both E1 and E2 are heavily glycosylated which contribute to the correct protein folding and execution of proper biological functions (Goffard et al., 2005). Additionally, there are eight cysteine residues that are highly conserved across all HCV genotypes which indicate a host of possible disulfide bonds between E1 and E2 (Castelli et al., 2017).

E2 is the major envelope protein that interacts with cell surface receptors and coreceptors with E1 possibly assisting in coordinating the entry process. However, the apolipoproteins that bind to the envelope proteins have also been shown to be crucial for entry (Lavie et al., 2006). It is currently believed that fusion is mediated by complex intra- and intermolecular E1E2 interactions, which coordinate structural and conformational rearrangements, exposing the fusion peptide (Vieyres et al., 2014). Compared to fusion and entry, much fewer studies have been conducted with regards to the role of E1/E2 in morphogenesis. However, it has been suggested that the envelope proteins undergo disulfide bond modification during the assembly process (Castelli et al., 2017).

1.5.2 Core protein

The core protein of HCV is similar to the capsid protein of flaviviruses in that it is a highly basic, RNA-binding protein. The protein varies in size from about 17-23 kDa with the 21 kDa core being the predominant form (Yasui et al., 1998). The core protein consists of three different predicted domains: an N-terminal hydrophilic domain (DI), a C-terminal hydrophobic domain (DII), and a signal peptide for E1. Like flaviviruses, the core exists in both membrane-bound and membrane-free, dimeric and multimeric forms. In addition to association with ER membranes and viral capsid formation, the core interacts with several other cellular proteins and pathways which may be crucial in the viral life cycle (Shimoike et al., 1999).

1.5.3 Nonstructural proteins

The nonstructural region of hepaciviruses consists of p7, NS2, NS3, NS4A, NS4B, NS5A, and NS5B which each mainly deal with replication and assembly. p7 is a small membrane protein that appears to be essential, but its exact function is yet to be defined. Some studies suggest it acts as a calcium ion channel and belongs to the viroporin family (Gonzalez et al., 2003). NS2 contains two internal signal sequences which are mainly responsible for ER membrane association (Santolini et al., 1995). NS2, along with NS3, forms the NS2-3 protease which self-cleaves from the complex and is eventually degraded. NS3 performs multiple functions in the viral life cycle, and its domains include the aforementioned serine protease at its N-terminus and a helicase/NTPase at its C-terminus. Additionally, NS3 interacts with NS4A to form another protease which is critical for the HCV life cycle and a major target for HCV therapeutics (Chatel-Chaix et al., 2010). NS4B is a membrane protein with at least four transmembrane domains responsible for anchoring and, additionally, can modulate NS5B RdRp activity (Chevaliez et al., 2006). NS5A mainly plays a role in replication and regulation of cellular pathways but the exact mechanisms by which it does so are fairly unclear. Finally, as mentioned above, NS5B is the viruses RdRp, catalyzing the synthesis of HCV RNA.

1.6 Protein and epitope tags

The study of viruses and their interaction with their host and environment can be particularly difficult without the use of tools to more efficiently detect and track certain molecules. Therefore, protein and epitope tags have been developed to aid researchers in more targeted studies. Currently, a wide range of protein and epitope tags are employed by researchers for many different reasons including detection, quantification, purification, and the identification of binding partners. For the purpose of this review, protein tags will refer to those with more than 12 aa (usually with some kind of structure) i.e. Green fluorescent protein (GFP), Renilla luciferase; and epitope tags will refer to tags with less than 12 aa i.e. FLAG, polyhistidine tag (HIS).

1.6.1 Luminescent tags

Fluorescent tags, among the most common biological tools utilizing luminescence, are protein sequences that fold and become fluorescent either through the formation of a fluorophore or by binding to a small molecule fluorophore. Other luminescent tags also emit a detectable and quantifiable light but do so through the use of enzymes and substrates. Luciferase is a common enzyme used in protein tags which catalyzes the oxidation of specific substrates resulting in the emission of a photon. These tags have revolutionized cell biology and changed the way cells are imaged and the information that can be gleaned from cell imaging. These tags can be fused to proteins of interest via genetic insertion which enables multicolor imaging with colors spanning the visible spectrum. Additionally, luminescent proteins can be affixed to RNA or DNA sequences in order to further interrogate biological processes.

The most common and widely used example of an intrinsically fluorescent protein is GFP. GFP is a 238 aa protein composed of an 11-stranded β -barrel which autocatalytically forms a fluorophore. All intrinsically fluorescent proteins share a similar fold and mechanism (Kremers, 2011). Depending on the protein, the fluorescence can last anywhere from minutes to days. Originally isolated from the *Aequorea* jellyfish, GFP has since been genetically inserted and expressed in a wide array of viruses, including flaviviruses, to study protein-protein interactions, conformational changes, and localization.

Many other fluorescent proteins have been derived from natural fluorescent organisms such as the sea anemone *Discosoma striata*, from which the commonly used protein tag DsRed was derived. However, this protein often exists as a tetramer and the isolation of monomers has proven to be very difficult (Campbell et al., 2002). Monomers are generally preferred for a number of reasons, one of the most important being the resulting size of the inserted gene. Inserting foreign genes into viral proteins can often lead to the excision of these genes during the replication and life cycle of the virus or, revertants, which lead to changes in the wild type genetic sequence (Thorn, 2017). One of the most successful and useful monomeric fluorescent proteins is mCherry which emits at around the 610 nm wavelength. Demonstrating stable and bright fluorescence, mCherry has a similar barrel architecture and shares the approximate dimensions of GFP derivatives but tends to have more elliptical symmetry. Although these tags have proven useful for live cell imaging, luciferase tags have also been utilized for their high sensitivity and ability to be adapted for high-throughput studies.

Renilla and Firefly luciferase are just a few of the commonly utilized luciferase tags that researchers use as reporters. Isolated from the sea pansy and firefly beetle, respectively, the tags utilize a chemical reaction to emit light that is often short-lived but highly correlative to the amount of tagged protein. Some of the most common uses for these tags are luciferase reporter assays which can be used to investigate the effect of regulatory elements like promoters, enhancers and UTRs, or the effect of mutations on gene expression (McNabb et al., 2005). These tags have proven useful in probing certain aspects of the viral life cycle but do not provide an efficient method to isolate and purify viral proteins for structural studies.

1.6.2 Affinity tags

Many of the first affinity tags used for protein expression and purification were large proteins developed for *E. coli*. Since then, advances in commercially available expression systems have fostered improvement on these original protein fusion partners. These new tools allow for the isolation of increasingly smaller, and more difficult to purify, viral proteins through affinity chromatography and other antibody or enzyme-based methods. Of the many purification tools used by researchers, a few of the most common are the HIS, FLAG, and Streptavidin (STREP) tags.

The HIS tag typically consists of six consecutive histidine residues but can sometimes vary in length from two to ten. Insertion of the small epitope tag rarely effects protein function and immunogenicity is typically conserved depending on the insert location. Histidine purification has become fairly ubiquitous and works via the formation of coordination bonds with immobilized transition metal ions. Depending on the protein being purified, immobilized Co^{2+} , Cu^{2+} , Ni^{2+} , Zn^{2+} , Ca^{2+} , and Fe^{3+} have all been used with Ni^{2+} being the most common (Kimple et al., 2013). A typical method of purification using the HIS tag is chromatography with metallic beads, but, various matrices can be utilized. Additionally, primary antibodies have been developed for detection of HIS tag fusion proteins *in vitro*.

The FLAG tag is similar to the HIS tag in size but differs in composition, making it more suitable for different types of antibody-mediated detection and purification. The FLAG tag is a hydrophilic affinity tag that can vary slightly in composition but typically consists of DYKDDDDK (D=aspartic acid, Y=tyrosine, and K=lysine). Similar to HIS tag, FLAG is small in order to avoid disruption of the native folding of proteins. The tag is also water soluble and works with a relatively inexpensive and efficient affinity purification procedure. The specific residues were chosen because aromatic aa are major factors in antigen-antibody interactions (Janeway et al., 2000). A Tyr was placed in the second position and flanked by highly charged aa because an aromatic amino acid is more likely to be involved in antigenic sites compared to less polar environments. The Lys at position three ensures maximum hydrophilicity and also contributes to the strong antigenicity.

There are currently several robust monoclonal antibodies available for the FLAG tag that enable Western blots, ELISAs, and a litany of other experiments to be performed with FLAG tagged proteins. Although both HIS and FLAG purification have been utilized for flavivirus and hepacivirus purification, there are also biotin-based tags that have been shown to be more efficient in some cases (Catanese et al., 2013).

The STREP tag utilizes the high-affinity interaction between biotin and streptavidin or avidin. The Strep- and Strep II-Tag, produced by Sigma, are 8 and 9 residue epitopes that can bind to a specific form of streptavidin. A major advantage of using the Strep-II tag is that protein-folding and secretion are mostly unencumbered. Another advantage of Strep-tagged proteins is that they can be isolated through one step affinity chromatography, and the binding affinity is particularly high which enables larger scale purification. Variations of the number of STREP

epitopes and their orientation can be engineered using linkers and spacers which increase the accessibility of the tag.

1.6.3 HiBiT reporter system

In order to address some of the barriers faced by the bulkier luminescence tags, Promega has recently developed the HiBiT detection system. HiBiT is a split reporter tag consisting of an 11 aa peptide which is fused to a protein of interest. The recombinant protein is then incubated with LgBiT, a 156 aa protein, which binds to HiBiT with an affinity of 0.7 nM. Upon binding, the complex emits a stable, glow-type luminescence measured at 470nm that is directly proportional to the amount of HiBiT-tagged protein (Promega, 2017). This allows for the creation of a standard curve that would simplify quantitation of proteins and virus particles by being able to correlate a luminescent signal with a certain level of expression/production. The HiBiT complex creates an enzyme that utilizes the substrate furimazine to create a signal that can be detected by a luminometer for hours, even with low abundance proteins at endogenous levels of expression. The resulting luminescence is relatively temperature and pH-stable but the background signal can vary depending on cell line and media used. The HiBiT kit comes in both a lytic and extracellular detection format and can be used for both protein detection and quantification as well as identifying protein-protein interactions. Thus far the HiBiT tag has been used to investigate proteins that are not readily tolerant of larger insertions.

With the development of HiBiT, researchers have been able to insert reporter genes into selected viruses from the family *Flaviviridae* such as DENV and HCV (Tamura et al., 2018). Nonstructural proteins in *Flaviviridae* have been shown to be tolerant of the HiBiT insertion with only a slight decrease in viral titer. However, when attempting to insert the gene into the structural region such as E protein, the viral titer decreases significantly (Tamura et al., 2019). Additionally, work has been done with West Nile virus like particles (VLPs) and subviral particles (SVPs) demonstrating the ability to study viral entry and release using HiBiT (Sasaki et al., 2018). HiBiT is still a fairly new system, but the current research serves to show that it can be utilized effectively in *Flaviviridae* and has a good chance of avoiding misfolding, altering dynamics, or inhibiting replication - some of the common problems that other luminescent reporter tags face.

CHAPTER 2. GENERATION AND CHARACTERIZATION OF REPORTER FLAVIVIRUSES

2.1 Chapter Summary

The previous chapter provided a broad overview of flaviviruses, their life cycle, pathogenesis, and clinical significance. Also introduced was the flavivirus genome and the 10 viral proteins that compose the particle and its replication machinery. Additionally, several different protein tags were discussed and a brief overview of the HiBiT system was provided. This chapter will delve into the methodology of integrating the HiBiT reporter tag and other reporters into the flavivirus genome and the characterization of the resulting recombinant virus. Previous efforts to tag flaviviruses with a wide range of tags are reviewed and many of the top sites and insert variations are described and assessed through titration, luminescence, and protein expression. Analysis of tag sites and construct variations in the DENV model system revealed two sites (one in C protein and one in M protein) capable of producing infectious virus when tagged with HiBiT. Although the recombinant virus containing HiBiT within M protein was found to be unstable after serial passaging, the C protein tagged DENV was stable over three serial passages. Furthermore, the HiBiT signal was found to directly correlate with purified infectious particles, indicating the retention of the capsid membrane anchor in assembled virus. Despite not producing infectious particles when tagged with HiBiT, sites in E protein were explored further and results showed that inserting tags other than HiBiT enabled production of infectious particles. This extensive analysis of HiBiT epitope insertion within DENV serves as a foundation for future studies attempting to create reporter viruses and hints at the possibility of a luminescent reagent that can be used to facilitate virus quantification and the study of DENV structural proteins.

2.2 Introduction

The flavivirus genus consists of positive-sense single stranded RNA viruses and includes important human pathogens such as Zika virus (ZIKV), Japanese encephalitis virus (JEV), and dengue virus (DENV) (Mukhopadhyay et al., 2005). All members of this genus encode 3 structural proteins and 7 nonstructural proteins that comprise the viral particle and replication proteins respectively. Viral assembly occurs on the membrane of the endoplasmic reticulum (ER), but

important conformational changes must occur before the particle matures and becomes infectious upon release (Apte-sengupta et al., 2014). Many of these conformational changes that occur throughout the life cycle of flaviviruses are poorly understood. Therefore, developing tools to study the complex dynamics of the flavivirus structural proteins is of particular importance.

Since the discovery of green fluorescent protein (GFP) in 1960, reporter proteins have revolutionized the way researchers investigate biological processes such as gene expression, protein localization, interaction, signaling pathways, and trafficking (Chalfie et al., 1999). As virus research has progressed, other bioluminescent proteins have been developed to conduct more targeted studies. For example, luciferase enzymes such as Renilla and Firefly are reporter proteins that have enabled highly specific and quantifiable light outputs. The incorporation of such reporter proteins into flaviviruses could prove crucial for the research of viral life cycle, pathogenesis, and the development of therapeutics. However, incorporating reporter tags into the structural region (C, prM/M, and E) of flaviviruses can be difficult due to the size of most reporter proteins causing misfolding, altering dynamics, etc. Additionally, many of the cDNA clones containing reporter genes are deleterious for bacteria (Ruggli et al., 1999).

In order to overcome these issues, Promega has recently developed a split luciferase system (HiBiT Protein Tagging System) involving a 1kDa protein (HiBiT) attached to a protein of interest that binds to a 156 amino acid, 17.6 kDa protein (LgBiT) with an affinity of 0.7 nM. After binding, the complex emits a sensitive and specific, glow-type luminescence upon addition of substrate. Thus far researchers have been able to develop recombinant flaviviruses possessing HiBiT within NS1 (one of the five nonstructural proteins of flaviviruses), which exhibited approximately a log decrease in focus forming units compared to wild type (Tamara et al., 2018). Work has also been done with West Nile SVPs and VLPs examining a detectable luminescent signal when incorporating HiBiT into the transmembrane region of E protein (Sasaki et al., 2018). However, a full-length, wild type titer flavivirus containing HiBiT within the structural region of the genome has yet to be described. Depending on the location of the incorporated HiBiT, such a reporter virus could be used to study the structural changes of flavivirus particles throughout their life cycle, such as the folding that occurs during maturation or dynamics that occur during viral breathing (Kuhn et al., 2015). Additionally, due to HiBiT signal being highly correlative to the amount of tagged protein, a reporter flavivirus containing the HiBiT gene could be used to simplify the quantification of virus production, saving researchers' time and resources in future studies.

2.3 Materials and methods

2.3.1 Cell culture

Baby hamster kidney (BHK-15) cells were cultured in minimal essential medium (MEM) supplemented with 10% fetal bovine serum (FBS) with 5% CO₂ at 37°C

2.3.2 Site-directed mutagenesis

The recombinant constructs were created using site-directed mutagenesis performed on full length DENV cDNA (serotype 2 strain 16681) following a modified Phusion polymerase protocol (New England Biolabs, NEB). Complementary, overlapping primers were designed using NEBuilder software and used for insertions of up to 57 bp. Following the polymerase chain reaction (PCR), products were digested using *DpnI* (NEB), phosphorylated using T4 polynucleotide kinase (NEB), and ligated using T4 DNA ligase (NEB). Mutants were transformed into DH5 α cells and plasmid DNA was extracted and sequenced through either Genewiz or the Low Throughput Purdue Genomics Core Facility. Following sequence confirmation, an approximately 3 kb segment of the full-length DENV cDNA mutant was created using the *SacI* and *KasI* restriction enzymes and gel purified using the gel extraction kit (Qiagen). The mutated segment was then ligated at a 1:1 molar ratio with the wild type (WT) cDNA that had been restriction digested using the enzymes described above and the appropriate segment (~11 kb) gel purified.

2.3.3 In vitro transcription and transfection of vRNA

Plasmid clones were linearized using the *XbaI* enzyme, in vitro transcribed using T7 RNA polymerase and cap A (NEB) at 37°C for 1.5 hours and run on a 0.8% agarose gel to confirm RNA product size and quality. Transfection into BHK cells was performed via electroporation using 0.2 cm gap cuvettes (BioRad). 18 micrograms of RNA for both WT and mutants were electroporated into cells using the following settings: 1.5kV, 25F, 200 Ohms and 2 consecutive pulses. Transfected cells were resuspended in 5% FBS MEM in both a 6-well and 96-well format for downstream collection (6-well) and HiBiT assays (96-well). Virus supernatants and lysates

were harvested at 24-hour timepoints up to 120 hours post electroporation (hpe) and stored at -80°C.

2.3.4 HiBiT assay

HiBiT activity was assessed using the HiBiT lytic detection kit and protocol provided by the manufacturer (Promega). Luminescence was measured with an integration time of two seconds at 470 nm in white polystyrene non-binding 96-well plates (Corning).

2.3.5 Plaque assay

Supernatant from the mutant and WT transfected cells were collected at 24-hour timepoints post transfection. BHK cells were plated in a 6 well format and 6, 10-fold dilutions of supernatant with PBS were used for infection once cells reached 90% confluency. Plates were rocked for 1 hour at room temperature and were then overlaid with 3 ml of a 1% agarose and 1X MEM mixture. The plates were then incubated at 37°C for 5 days. After day 2, 2 ml of 5% FBS MEM was added to each well to prevent the agarose from drying. Each well was then stained using a neutral red solution and counted to determine viral titer.

2.3.6 Infections

BHK cells were infected with DENV recombinant mutants and WT DENV at an MOI of 0.01 at room temperature and gently rocked for 2 hours. After rocking, the virus supernatant was aspirated and replaced with MEM supplemented with 2% FBS. The infected cells were incubated at 37°C and supernatant was collected at 24-hour timepoints and replaced with new media. Infections continued for up to eight days depending on observed CPE.

2.3.7 Density gradient centrifugation

Supernatant of transfected cells was collected at 24-hour timepoints and pooled together. Total sample was spun at 32,000 RPM for 2 hours at 4°C with a 24% sucrose cushion using the Optima L-100 XP ultracentrifuge and type 50.2 rotor (Beckman Coulter). Concentrated virus was applied to the top of a linear gradient formed from 10-35% solutions of potassium tartrate and glycerol. Gradient was spun at 32,000 RPM for 2 hours at 4°C using an SW41 rotor (Beckman

Colter). Fractions were extracted from bottom to top using 500 μ l increments and the HiBiT activity and infectious titer was assessed for each fraction.

2.3.8 SDS-PAGE and western blot

Transfected or infected cell supernatants and lysates were collected at 24-hour timepoints. Cells were lysed through the addition of 250 μ l of RIPA buffer. SDS-PAGE was performed using a 10% acrylamide gel with or without heating samples for 5 minutes at 95°C depending on the protein being visualized. Additionally, samples were mixed with loading dye and BME depending on whether reducing conditions were necessary. The nitrocellulose membrane was probed with anti-FLAG, 4G2, or anti-NS5 antibodies. Secondary antibodies with infrared-labels (680-800nm) were added to the membrane and visualization was done utilizing an Odyssey infrared imager (LICOR).

2.4 Results

2.4.1 Development of HiBiT methodology and replication of previous findings

Before attempting HiBiT insertion in the structural proteins of DENV, the cloning methodology was optimized in order to minimize the possibility of off-site mutations and obtain a nonstructural, HiBiT-tagged DENV control to compare with structurally tagged recombinant virus. After attempting to engineer the 33 amino acids (aa) that compose HiBiT via standard Phusion (NEB) protocol, the reaction failed to produce a viable PCR product. However, a modified Phusion (NEB) protocol utilizing blunt-end ligation was used to introduce the mutation and the product was able to be transformed and confirmed via sequencing. To validate the low possibility of off-site mutations, a mutation (K101-E101), discovered and evaluated by fellow lab mates and known to have no effect on viral titer, was introduced. The mutation was engineered using the previously described SDM methodology and confirmed via sequencing. The mutant DENV exhibited similar titer compared to WT with a peak viral titer of 3.2×10^5 PFU/ml compared to 3.8×10^5 PFU/ml respectively. When accounting for standard deviation, the difference between the two was not statistically significant ($p > 0.1$). Therefore, the cloning method most likely did not introduce off site mutations and was used for all future SDM reactions.

After validating the cloning method, two sites in NS1 of DENV (NS1-4 and NS1-349) were chosen to potentially serve as a positive control for HiBiT-tagged viruses. The NS1 sites were chosen in an attempt to replicate previous findings that demonstrated these sites can tolerate HiBiT insertion and experience only a one to two log decrease in WT titer (Tamara et al., 2018, Tamara et al., 2019). The NS1-4 HiBiT construct consisted of a repeat of the first four amino acids of DENV NS1 followed by the HiBiT insert and a GSSG linker at the C-terminus for added flexibility. The second site was characterized in JEV following amino acid 349 of NS1 and consisted of only the HiBiT insert. These exact constructs were engineered following methodology described above, with the NS1-349 tag site correlated to the analog amino acid in DENV NS1. The recombinant virus was then characterized through plaque assay and HiBiT assay. However, the recombinant virus did not yield an infectious titer comparable to WT as described in previous studies (Figure 2.1).

Previous studies found that inserting HiBiT after the fourth amino acid of NS1 in DENV serotype 4 yielded a peak infectious titer of $\sim 2 \times 10^4$ FFU/ml compared to a wild type infectious titer of 1×10^5 FFU/ml, indicating approximately a log decrease in titer (Tamura et al., 2018). Tamura et al. calculated infectious titer when the recombinant virus reached its peak titer at 120 hpi. The study also found the NS1-4 recombinant virus to display HiBiT activity of approximately 10^5 Relative Light Units (RLU) compared to WT DENV infected cells with a HiBiT activity of approximately 10^3 RLU, a 2-log increase. This study was replicated under slightly different conditions such as transfecting BHK cells and assessing via plaque forming units instead of focus forming units. Under these conditions, the NS1-4 HiBiT-tagged DENV reached a peak titer of 5.1×10^2 PFU/ml and displayed HiBiT activity of 6.7×10^5 RLU compared to a WT titer of 5.2×10^5 PFU/ml and HiBiT activity of 1×10^4 RLU (Figure 2.1). In addition to delayed growth kinetics compared to WT, the infectious titer of the recombinant NS1-4 DENV was not high enough in BHK cells to be used in downstream assays. The NS1-349 tag site also displayed lower infectious titer and HiBiT activity than previously described.

Along with site NS1-4 in DENV, Tamura et al. also characterized an NS1 C-terminal site at aa 349 in JEV. In the study, after five serial passages, Huh7 cells were infected with the mutant virus and this site was shown to have an infectious titer and growth pattern identical to WT and displayed HiBiT activity of 10^8 RLU at 48 hpi compared to a WT HiBiT activity of 10^3 RLU (Tamura et al., 2019). However, upon replicating this experiment with a DENV construct and

infection performed in BHK cells, the recombinant virus displayed an approximate 2 log decrease in peak viral titer and HiBiT activity of 6.9×10^6 RLU compared to a WT of 10^4 RLU (Figure 2.1). Similar to the NS1-4 site, NS1-349 HiBiT DENV did not display high enough titer compared to WT to be used as a positive control for HiBiT signal. However, these results confirmed the possibility of constructing an infectious recombinant DENV containing the HiBiT gene.

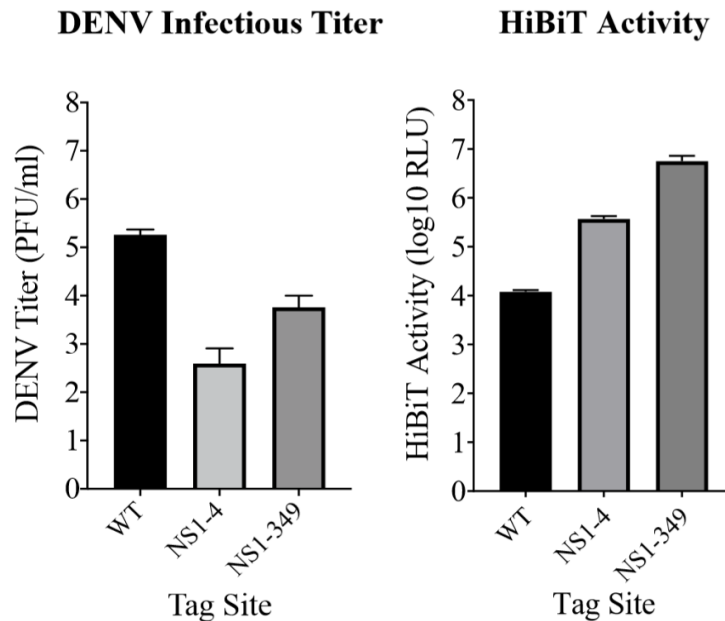


Figure 2.1. Evaluation of HiBiT recombinant DENV NS1 tag sites. BHK cells were electroporated with vRNA and supernatants were collected at 24-hour intervals. Displayed is the peak infectious titer for WT (96 hpe), NS1-4 (96 hpe), and NS1-349 (96 hpe) as assessed by plaque assay (left). The luminescence of the cell lysate from the timepoint corresponding to peak infectious titer was determined using HiBiT assay (right). Experiments were performed in triplicate.

2.4.2 Determination of suitable HiBiT loci and construct variation

In order to determine an ideal locus for HiBiT insertion, previous literature was analyzed for insertion sites of protein and epitope tags with similar size and/or composition compared to HiBiT. Additionally, the DENV structure was examined for flexible, surface exposed regions that may tolerate insertion. A total of 16 distinct loci in the structural region were chosen: one in capsid protein (C), three in membrane protein (M), and 12 in envelope protein (E). Depending on the previous literature and accessibility of the site, variants of the construct were created with either one linker sequence at the N-terminus of HiBiT or flanking linker sequences (Figure 2.2A).

Previous findings suggest C protein is tolerant of SmBiT and GFP11 insertion in its C-terminus, adjacent to the membrane anchor, with only a log decrease in WT titer (Eyre et al., 2017). The loops connecting the transmembrane alpha helices of both M protein and E protein have also been found to withstand HiBiT insertion in West Nile virus SVPs and VLPs (Sasaki et al., 2018). Finally, sites in domain I of E protein have been shown to tolerate FLAG epitope insertions without affecting fitness in ZIKV (Chambers et al., 2018). Additional sites in domain III of E protein were chosen due to their flexibility as a surface exposed loop or known capacity to bind to neutralizing antibodies which indicates possible space for HiBiT insertion (Gromowski et al., 2007, Oliphant et al., 2007) (Figure 2.2 B). To construct the HiBiT-tagged DENV, a full length DENV serotype 2 strain 16681 was used as a template.

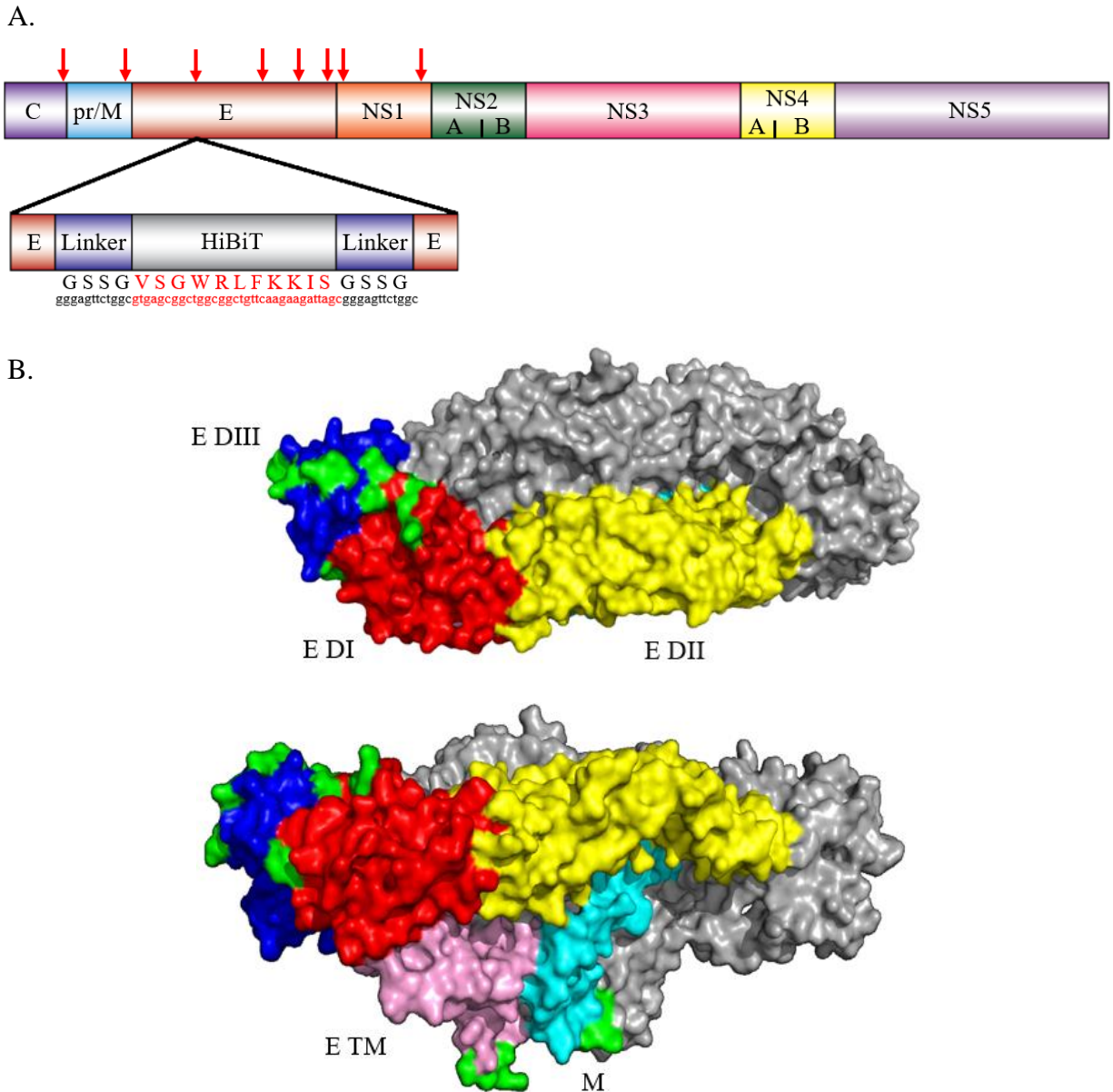


Figure 2.2. HiBiT loci position in genome and mature E-M structure. (A) A schematic representation of DENV and the sequence of HiBiT and flanking GS linkers within E protein. Red arrows indicate HiBiT insertion sites further described in table 2.1. (B) Structure of DENV E protein ectodomain dimer along the 2-fold axis (top) and side view showing transmembrane domains (bottom). E domains I (red), II (yellow), III (blue), and the transmembrane stem and anchor (pink). The M protein transmembrane, stem, and loop regions (cyan). Also displayed are the tagging locations for HiBiT insertion (green).

Table 2.1 DENV-HiBiT tag locations and construct variation. Table describing HiBiT tag locations with viral protein, protein region, nucleotide in full length genome, preceding amino acid within viral protein, and linker orientation specified

Protein	Protein Region	Amino Acid	Nucleotide	Linker Orientation
C	Transmembrane	103	439	None
M	Transmembrane Loop	54	907	None, Flanking, N-terminus
		55	910	None, Flanking, N-terminus
		56	913	None, Flanking, N-terminus
E	DI	147	1417	None, Flanking
		149	1423	None, Flanking
		150	1426	None, Flanking
		152	1432	None, Flanking
		156	1444	None, Flanking
E	DIII	296	1861	None, Flanking
		328	1954	None
		361	2053	None
		383	2119	None, Flanking
E	Transmembrane Loop	470	2380	None, Flanking, N-terminus
		471	2383	None, Flanking, N-terminus
		472	2386	None, Flanking, N-terminus
NS1	β -roll	4	2467	N-terminus
	β -ladder	349	3502	None

2.4.3 Characterization of recombinant DENV replication and translation competence

After constructing the recombinant flaviviruses carrying the HiBiT gene, the biological characteristics were assessed using a HiBiT screening methodology. Viral RNA was transfected into BHK cells and luminescence was measured at 48 hpe (Figure 2.3). 24-hour timepoints post electroporation were initially assessed using the HiBiT assay and 48 hpe was found to yield peak signal for a majority of the samples. All construct variants were subjected to electroporation and subsequent HiBiT screening at 48 hpe. However, the addition of GSSG linkers did not alter the signal by more than 0.5 log RLU for each respective sample. Therefore, the construct containing only the HiBiT gene was used for comparison of HiBiT activity between different tag sites. Luminescence of WT (lacking HiBiT) transfected cell lysate yielded a value of approximately 10^4 RLU which was used as a baseline to compare mutant cell lysate values. Apart from sites M-54

and E-328, all other sites displayed varying levels of HiBiT activity with a maximum value of approximately 10^8 RLU achieved by site E-152.

The tag site adjacent to the C protein membrane anchor yielded a signal of approximately 2×10^6 RLU. Sites in the E and M protein transmembrane loop, aside from M-54, displayed similar signals of approximately 10^6 RLU. On average, sites in domain I of E protein displayed the highest HiBiT signal with sites near the DENV glycosylation site and fusion loop of the adjacent E monomer (E-149, E-150, E-152) yielding a signal at or above 10^7 RLU. A luminescent signal above that of the WT indicated at least some level of transcription and translation due to HiBiT's ability to bind to LgBiT. According to the manufacturer, luminescent signal is directly proportional to HiBiT tagged protein over seven orders of magnitude. Therefore, deviation from the maximum value indicates some modification or inhibition of RNA transcription, translation of viral proteins, or accessibility of HiBiT and, thereby, its ability to bind to LgBiT. Future studies will need to be completed in order to determine the exact reason for the variability amongst HiBiT tag sites. However, any HiBiT tag sites displaying HiBiT activity above that of the WT were then subjected to a HiBiT infectivity screen.

HiBiT Activity 48 Hours Post Electroporation

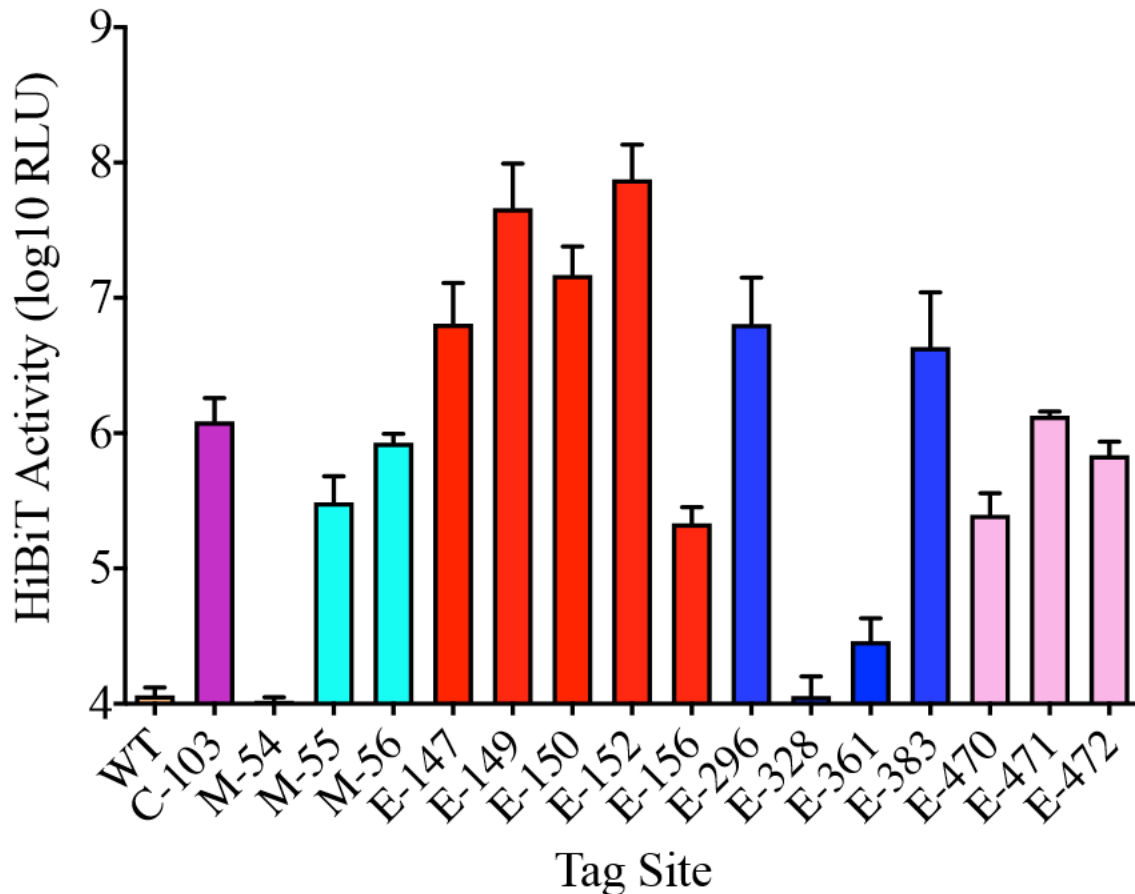


Figure 2.3. Luminescence of electroporated cells at 48 hours. Viral DENV RNA was transfected in BHK cells via electroporation and seeded in a 96-well plate format. At 48 hours post electroporation the cells were lysed with the HiBiT lytic reagent and luminescence was measured with an integration time of two seconds at 470 nm. Luminescence is measured in relative light units. The Y-axis begins at 10^4 RLU to account for WT HiBiT activity. Each experiment was performed in duplicate. Color scheme analogous to proteins and protein domains denoted in figure 2.2B with the addition of C protein in purple. Experiments were performed in triplicate.

2.4.4 Characterization of recombinant DENV infectious particle production

Following characterization of the recombinant DENV mutants post transfection, supernatant from electroporated cells was used for a first passage (P1) infection. Although the supernatant had not been titrated, the goal of this screen was to assess the ability of the virus to propagate HiBiT signal. To do this, 100 μ l of 48 hpe supernatant was incubated with BHK cells at 90-100% confluency in a 96-well plate. Two wells were infected for each sample and,

immediately following infection, the first well was lysed with the HiBiT lytic reagent and a 0 hpi luminescence value was measured. After 72 hpi, a second luminescence value was measured and compared to the 0 hpi value to determine any deviation from the baseline value. Again, all constructs and construct variants were subjected to the P1 screen, but the addition of linkers made little difference in the ability of viruses to produce infectious particles. Therefore, the construct with only the HiBiT tag was used for tag site comparison.

Of the 16 tag sites in the structural region, only two sites demonstrated an increase in HiBiT activity over 72 hours (Figure 2.4). Both sites C-103 and M-55 had approximately a log increase in HiBiT activity as compared to their 0 hpi timepoints. All other constructs experienced no change or a decrease in signal compared to their 0 hpi timepoints. Despite extensive washing with PBS, both after infection and before collection of cell lysates, some samples, notably E-149 and E-150, yielded high 0 hpi HiBiT activity compared to WT. Those samples with particularly high ($>10^5$) HiBiT activity at 0 hpi all had a decrease in signal with E-150 showing a nearly two log decrease. All samples were titrated via plaque assay but only C-103 and M-55 indicated infectious particles that maintained HiBiT were being produced.

HiBiT Activity 0-72 Hours Post Infection

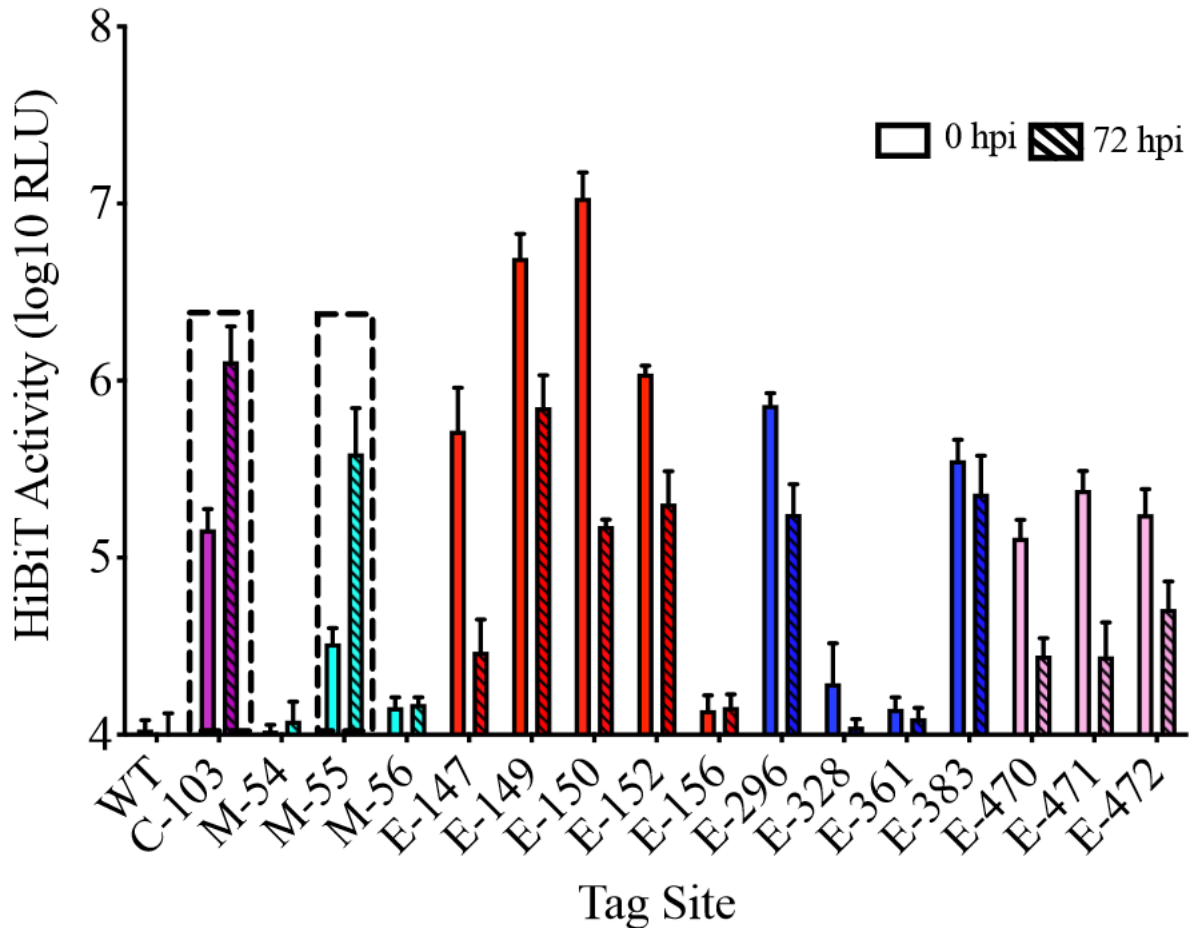


Figure 2.4. Luminescence of infected cells at 72 hours post infection. BHK cells were seeded in a 96-well format and infected with 100 μ l of virus supernatant from 48 hours post electroporation (see Figure 2.3) when the cells reached 90% confluency. The plates were washed extensively with pbs after rocking with virus inoculum for 2 hours. For “0hpi” samples, the samples were lysed immediately after PBS washing with the HiBiT lytic reagent. For “72hpi”, the infection proceeded for 72 hours before the samples were lysed and luminescence measured with a two second integration time at 470nm. Experiments were performed in triplicate.

To investigate the viral titer and growth kinetics of the mutant viruses, plaque assays and infections in BHK cells were performed. The supernatant of transfected virus was collected at 24-hour timepoints post electroporation and titrated. Although C-103 and M-55 both demonstrated slower growth kinetics, the viruses eventually reached their peak titer at 96 hpe at 6.1×10^3 PFU/ml and 1.8×10^3 PFU/ml respectively (Figure 2.5). All other titrated viruses displayed no visible plaques.

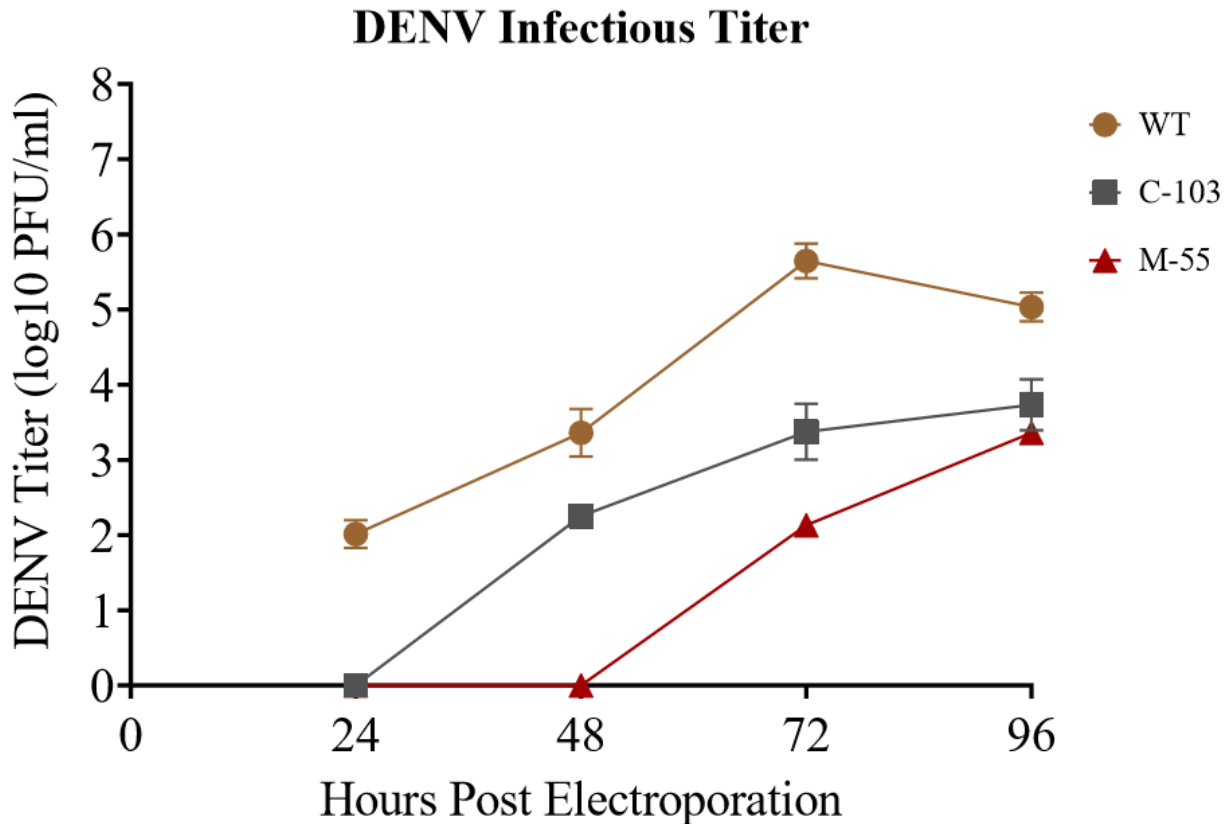


Figure 2.5 Infectious titer of recombinant clones following electroporation. BHK cells were transfected with WT, C-103, and M-55 vRNA and seeded in a 6-well format. Supernatant was collected at 24-hour intervals and infectious titer was assessed via plaque assay. Experiments were performed in triplicate.

After initial titration of transfected cell supernatants was performed, naïve BHK cells were infected with C-103, M-55, and WT DENV at an MOI of 0.01 and the infection progressed for up to 8 days. Viruses containing HiBiT inserted at site C-103 were stable over three cycles of infection and maintained its initial peak titer of approximately 7×10^3 PFU/ml after serial passaging (Figure 2.6). This titer represents a two log decrease as compared to WT DENV. Despite infectious titer stability, HiBiT activity was assessed at 120 hpi and was shown to be variable compared to the initial, P0 HiBiT assessment. Following the same infection procedure, M-55 seemed to yield WT titer after first round infection. Upon performing the HiBiT assay with supernatant from infected cells, an initial increase in HiBiT activity up to 72 hpi is followed by a steady decline down to WT levels (Figure 2.7).

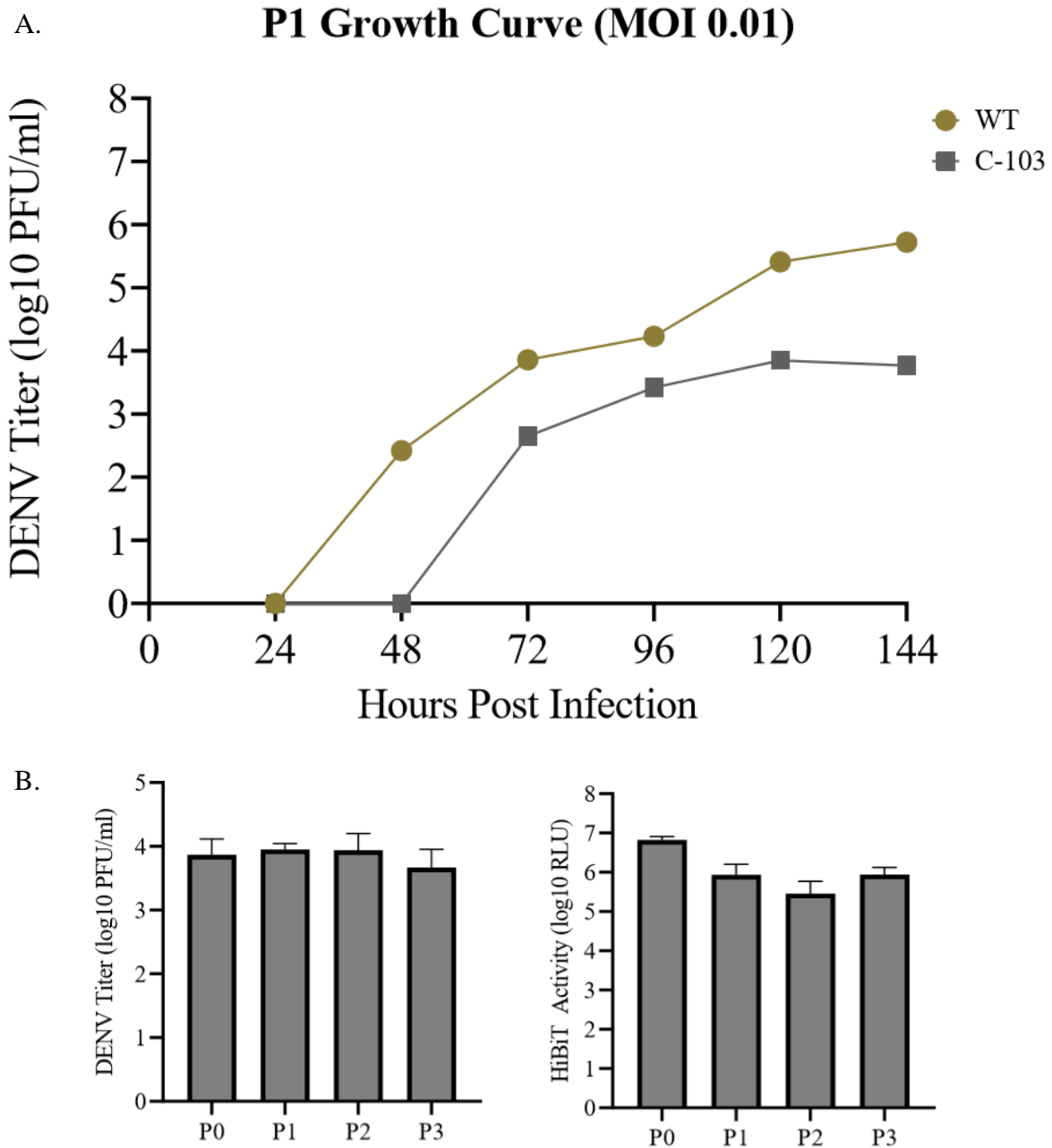


Figure 2.6 Infectious titer and HiBiT activity of C-103. (A) BHK cells were infected with WT and C-103 recombinant virus at an MOI of 0.01 in both a 6-well and 96-well format. Supernatant was collected at 24-hour intervals, cells were washed with PBS, and fresh media was added to each well. Infectious titer was assessed by plaque assay of the supernatant collected from the 6-well plate and HiBiT assay was performed with the lysate from the 96-well plate. (B) Supernatants collected from the previous passage were used to infect naïve BHK cells and the above procedures were repeated. Depicted are the titers and HiBiT activity at 96 hpe for P0 and 120 hpi for P1-P3 (peak titer).

P1 Growth Curve (MOI 0.01)

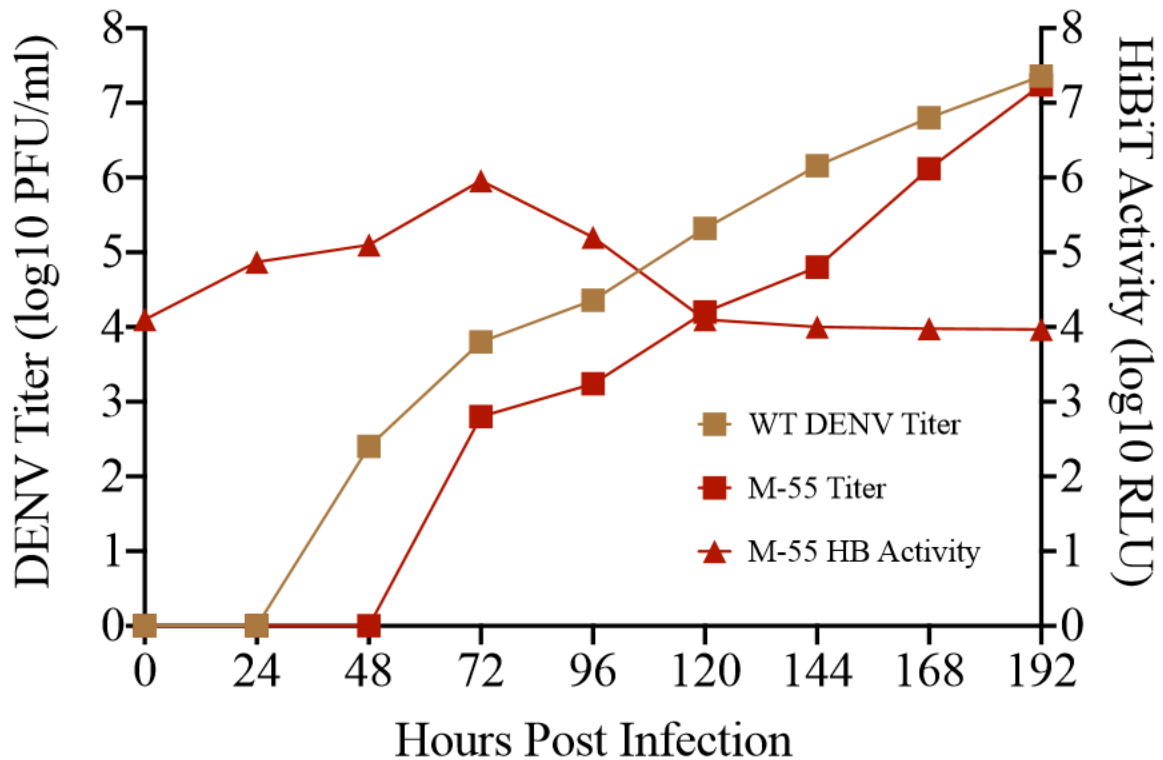


Figure 2.7 Infectious titer and HiBiT activity of M-55. BHK cells were infected with WT and M-55 recombinant virus at an MOI of 0.01 in both a 6-well and 96-well format. Supernatant was collected at 24-hour intervals, cells were washed with PBS, and fresh media was added to each well. Infectious titer was assessed by plaque assay of the supernatant collected from the 6-well plate and HiBiT assay was performed with the lysate from the 96-well plate. Infection proceeded for eight days.

2.4.5 C-103 HiBiT signal is associated with the DENV particle

The results from the growth curve of C-103 recombinant virus seem to suggest that the particle is retaining the tag and is stable throughout serial passaging. However, previous findings suggest that the $\alpha 5$ helix of C protein, the site of HiBiT tagging for this virus, is cleaved and retained in the ER. In order to investigate this, supernatant from electroporated cells was collected at 24-hour timepoints and purified using ultracentrifugation and a 24% sucrose cushion. Following purification, the resulting product was added to a potassium tartrate-glycerol gradient which consisted of 6 different densities (10-35%). After ultracentrifugation, the fractions corresponding to different densities were extracted and HiBiT assays were performed in parallel with plaque

assays for each fraction (Figure 2.8). Peak HiBiT activity was found to occur mainly at the fractions corresponding to 15 and 20% (9-15). Previous research has found that the DENV particle localizes within the 20% fraction (Yu et al., 2009). Infectious titer for each fraction was assessed and the peak HiBiT signal was found to associate with infectious particles. Fraction 11, which correlates to the 20% density, yielded the highest titer with approximately 1.2×10^3 PFU/ml and HiBiT signal of 2.0×10^5 RLU. Fractions 10 and 12, also correlating to the 20% density, were found to have slightly lower titers than fraction 11 and, subsequently, a lower HiBiT signal. Fractions 13 and 14, corresponding to the 15% density, also yielded infectious particles but maintained a similar HiBiT activity as compared to fraction 11. Fraction 15 and 16 demonstrated relatively high luminescent signal but were not found to contain infectious particles.

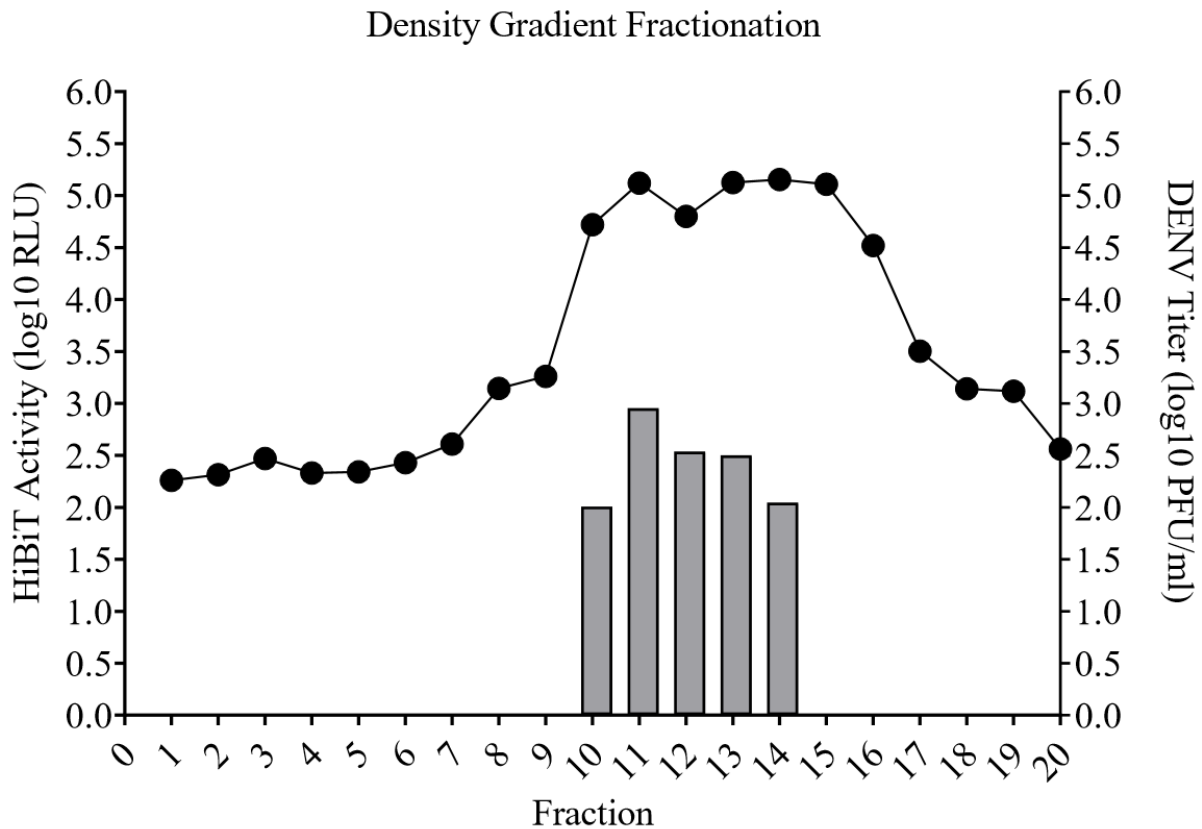


Figure 2.8 HiBiT activity and infectious titer for each fraction following density gradient fractionation. Supernatant from cells transfected with C-103 vRNA was collected at various timepoints and purified using a 24% sucrose cushion and ultracentrifugation. Purified supernatant was then added to a potassium-tartrate, glycerol gradient and spun for 32,000 RPM for two hours. 500 μ L fractions were extracted from bottom to top and each fraction was assessed for HiBiT activity (line) and infectious titer (column) via HiBiT and plaque assay respectively.

2.4.6 Composition of insert within E protein is critical for infectious particle production

The HiBiT assay performed at 48 hpe displayed a wide range of HiBiT activity amongst tag sites. However, the sites within domain I of E protein, on average, yielded a much higher signal compared to the rest (Figure 2.3). Despite the high HiBiT activity following transfection, upon using the 48 hpe supernatant to infect naïve BHK cells, the EDI recombinant mutants were unable to make infectious particles. In order to investigate the discrepancy between high HiBiT activity following transfection and an inability to propagate HiBiT to new cells, different epitope tags were inserted in tag site E-149, a representative of the EDI tag sites. Site E-149 had previously been shown to tolerate FLAG epitope insertions, aa sequence: DYKDDDDK, with little to no effect on infectious titer in ZIKV (Chambers et al., 2018). Additionally, SmBiT (Promega) aa sequence: VTGYRLFEEIL, an alternative to HiBiT, shares a similar size compared to FLAG and HiBiT but has a different amino acid composition. These two tags were engineered into site E-149 with the hope of rescuing infectivity. The recombinant clones were then transfected, and the resulting supernatant was titrated (Figure 2.9).

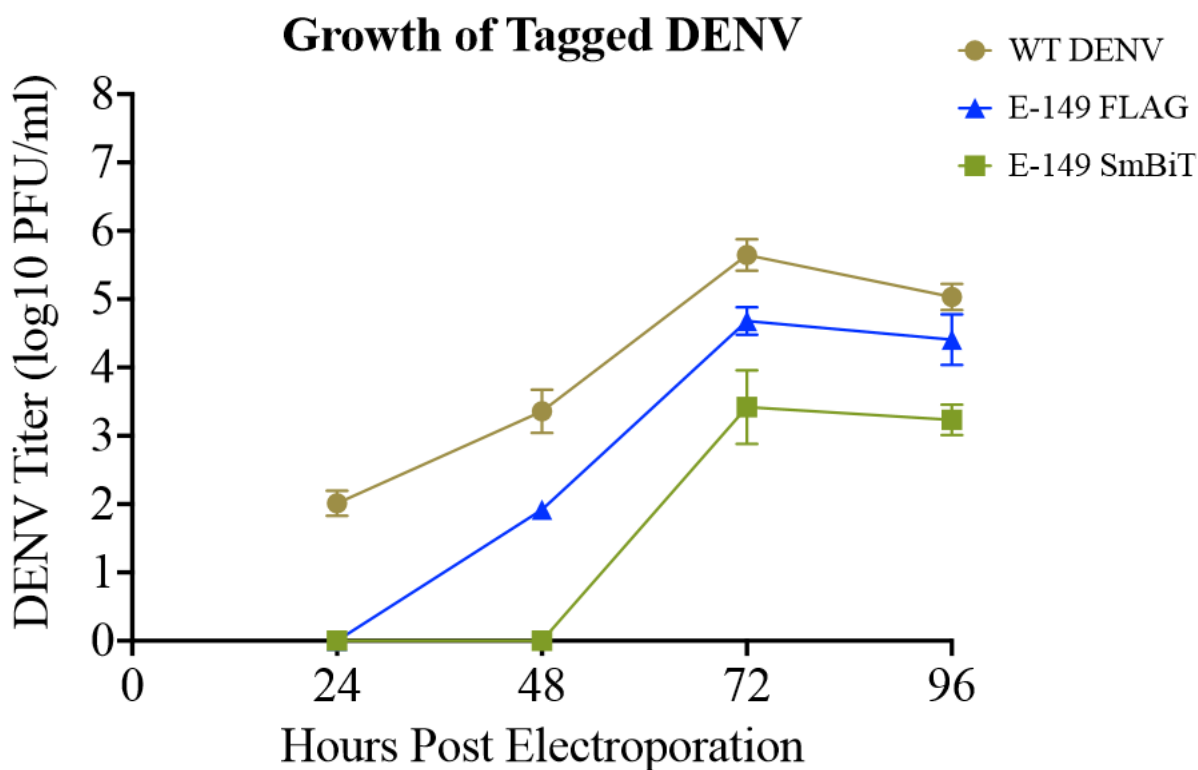


Figure 2.9 Infectious titer of recombinant virus containing FLAG and SmBiT epitopes. BHK cells were transfected with WT, E-149 FLAG, and E-149 SmBiT vRNA and seeded in a 6-well format. Supernatants were collected at 24-hour intervals and infectious titer was assessed via plaque assay. Experiments were performed, with biological replicates, in triplicate.

Supernatant and lysis were collected at 24-hour timepoints post electroporation and FLAG expression was confirmed through western blotting using anti-FLAG antibodies. The HiBiT assay was also performed with the E-149 SmBiT clone and HiBiT activity was found to be approximately 7×10^5 RLU at 72 hpe, confirming SmBiT expression. Both the FLAG and SmBiT insertions were able to rescue infectivity, with the E-149 FLAG mutant demonstrating a peak viral titer of 4.4×10^4 PFU/ml at 72 hpe and SmBiT with a titer of 3.3×10^3 PFU/ml at 72 hpe. Despite FLAG and SmBiT displaying an approximate one and two log decrease in infectious titer respectively, the ability to rescue any infectious titer by replacing HiBiT demonstrates that composition, and not necessarily size, of the tag is crucial for infectious particle production.

2.5 Discussion

In order for a HiBiT-tagged DENV to be used as a reagent for future studies, the recombinant virus must behave as closely to WT as possible. This includes near identical titer, growth kinetics, and plaque morphology. Before choosing sites in the structural proteins of DENV to achieve the aforementioned objectives, two sites that had previously been described to tolerate HiBiT insertion with minimal loss in infectivity were constructed and characterized. Sites NS1-4 and NS1-349 had been characterized in DENV serotype 4 and JEV respectively (Tamara et al., 2018, Tamara et al., 2019). After constructing and characterizing the recombinant virus, the HiBiT tag sites were found to maintain infectivity and emit luminescence. However, the clones did not achieve an infectious titer within one log of WT DENV2 and, therefore, could not be used as a positive control to compare against HiBiT tag sites in the structural region (Figure 2.1). Only the construct variants described in the published studies were attempted; but recent studies, and results within this study, indicate that insert composition may be critical for the maintenance of WT virus replication competency and infectivity (Eyre et al., 2017). Eyre et al., also demonstrated that tags within NS1 impaired virus replication efficiency which may have contributed to the deficiency in viral titer. Following the characterization of sites in NS1, using previous studies and the structure of the virion as a guide, sites were chosen in the structural proteins (C, M, and E) that were believed to be able to tolerate HiBiT insertion.

The structural proteins of flaviviruses play many important roles in flavivirus infection and pathogenesis (Apte-Sengupta et al., 2014). Therefore, choosing sites to tolerate HiBiT insertion without inhibiting WT replication and infectivity proved to be a serious challenge. Sites were chosen that avoided the β -sheet and α -helices of E and M, which are common structural elements of many different proteins and typically possess a wide range of functional or stabilization roles (Richardson, 1981). Furthermore, previous studies have shown the ability of SVPs, VLPs, and full-length flaviviruses to tolerate insertions anywhere from a few amino acids in length to full size fluorescent proteins (Evans et al., 2018, Eyre et al., 2017, Sasaki et al., 2018, Tamara et al., 2018, Tamara et al., 2019). The sixteen sites chosen were constructed with varying construct modifications like GS linkers on one or both termini that have been shown to increase flexibility and stability of tagged viruses (Chen et al., 2013). The initial HiBiT screen was performed to assess replication and translation competency and, as expected, the constructs showed a wide range of HiBiT activity (Figure 2.3). Aside from sites M-54 and E-328, all other sites displayed HiBiT

activity above that of WT with sites E-149 and E-152 displaying the highest activity. The variation in HiBiT signal could be due to a number of factors including replication deficiency, improper folding, or general accessibility of the tag. Although the cells were lysed prior to incubation with LgBiT, aggregation of proteins and location of HiBiT within the tagged protein could have affected the binding capacity of HiBiT to LgBiT (Dixon et al., 2016). Despite some clones showing little activity post electroporation, all recombinant clones were subjected to an infectivity screen.

Only tag sites M-55 and C-103 were capable of infecting a fresh batch of BHK cells and propagating HiBiT signal, both exhibiting an approximate two log decrease in peak infectious titer compared to WT (Figure 2.4, 2.5). All other sites that displayed replication and translation competency had a decrease in HiBiT signal over time in the infectivity screen, suggesting the virus may be defective in assembly, maturation, or fusion. Further studies must be done to assess the exact reason for the loss of infectivity. That being said, epitope insertions in E-149 seem to suggest that the composition of the tag contributes to infectious particle production, at least within domain I of E protein. The sites within EDI are near the fusion loop of the adjacent E monomer (Chambers et al., 2017). The structure of HiBiT and SmBiT is not yet known but FLAG has little to no structure. FLAG tag was able to be inserted in site E-149 and produce infectious particles with little decrease in infectious titer compared to WT (Figure 2.9). A possible explanation as to why HiBiT is unable to be inserted in the EDI region, while FLAG and SmBiT are, could be that the structure of the inserted reporter tag occludes the fusion loop, thus preventing fusion. Another possible explanation as to why SmBiT and FLAG insertion was able to rescue infectious particle production is the importance of negative residues in this particular region of the E/M dimer. FLAG is highly charged and seems to have little effect on DENV replication, folding, assembly, and fusion (Kimple et al., 2013). Regardless of the reason for inhibition of infectivity for some clones, the two tag sites that exhibited particle production were further characterized to assess stability and growth kinetics.

Tag site C-103 demonstrated stable titer but varied HiBiT activity across three infections. What's interesting about this tag site, and the resulting possibilities regarding its use as a reagent to study DENV, is its position within the C protein signal peptide. The DENV polyprotein is cleaved at the COOH terminus of C protein and the viral proteases that catalyze this cleavage are recruited to the site through a signal peptide (Stocks et al., 1998). Capsid consists of an N-terminal, positively charged loop followed by five α -helices with helix α -5 being the signal peptide directing

the translocation of prM through the ER. All previous structures of flavivirus capsid seem to indicate C protein exists in its signalase cleaved form, N-terminus to the end of helix α -4, within the particle (Ma et al., 2004). However, a recent study suggests, through structural and MALDI-TOF analysis, that flaviviruses may retain helix α -5 in assembled virions (Tan et al., 2020). Furthermore, the helix may serve an important role in assembly by facilitating interactions amongst capsid dimers. Tan et al. also found that assembled flavivirus particles exist as a heterogeneous population with both C proteins that retain the α -5 helix and those that do not.

Although a stable infectious titer was observed in this study, the HiBiT activity varied depending on the passage (Figure 2.6B). If HiBiT is truly directly correlative to the amount of tagged proteins present within the cell lysis, it is expected that the observed HiBiT activity would also be stable throughout serial passaging, assuming a stable amount of tagged protein. The results in this study seem to support the notion of a heterogeneous population of both cleaved and partially cleaved C protein amongst flavivirus particles. This notion is further supported by peak HiBiT signal associating with infectious titer following density gradient centrifugation (Figure 2.8). Although there is detectable signal in fractions without infectious titer, this could be due to a number of factors including noninfectious particles including the helix α 5, difference in matrix affecting luminescent detection, or inefficient fraction extraction. However, if HiBiT is directly associated with infectious particles, then helix α 5 must be retained in at least a fraction of the virus population. The difference in HiBiT signal across generations may be attributed to a possible degradation of cleaved signal peptides and a retention of helix α 5 in the ER as well as uncleaved C protein incorporated in the virus particle. A slightly inhibited titer when tagging helix α 5 of C protein with HiBiT can also be explained due to possible inhibition of its role in virus assembly or partial inhibition of NS2B/NS3 cleavage. The retention of HiBiT in site C-103 suggests that the structure and composition of HiBiT does not irreparably alter the interactions facilitated by helix α 5, or, that the remaining population of cleaved C protein is enough to compensate for the interactions HiBiT may disrupt. Regardless, a HiBiT-tagged C protein signal peptide provides a useful tool to study maturation and assembly as well as tracking the presence and absence of helix α 5 throughout the flavivirus life cycle.

Upon serial passaging recombinant M-55 virus, WT titer was rescued and HiBiT activity returned to WT levels over the course of the first passage. There are a few explanations for this. First, the virus could have reverted to its WT composition, likely beginning at 72 hpi which is

where the drop in HiBiT activity is first characterized (Figure 2.7). The reversion would most likely be the excision of the entire tag but could also be a partial excision that resulted in the prevention of HiBiT-LgBiT binding (Dixon et al., 2016). Another explanation could be that a mixed population of both WT and recombinant RNA, because of incomplete digestion of WT DNA during cloning, was transfected into BHK cells and, due to some sort of inhibition of the virus because of HiBiT insertion, the WT virus outcompeted the recombinant virus during infection. The first scenario indicates that the recombinant virus is unstable and, therefore, cannot be used as a tool to further study DENV. The second scenario could potentially be addressed by purifying M-55 recombinant virus and repeating infection. This would ensure a homogenous virus population and could help identify the exact reason for a loss of HiBiT signal. After determining the cause of the decreased HiBiT signal, additional serial-passaging and luminescence analysis should be completed to evaluate the usefulness of the M-55 tagged virus as a reporter.

The establishment of a flavivirus that emits a quantifiable luminescence would be particularly helpful in the quantification of virus production and could be used for a wide array of studies including those investigating replication, entry, and protein interactions (Schwinn et al., 2017). After construction and characterization of 16 individual sites with varying insert compositions, sites M-55 and C-103 maintained infectivity and could prove useful as tools to further examine different aspects of the flavivirus life cycle. These findings serve as a foundation for further studies, of both RNA and DNA virus families, that wish to engineer recombinant viruses. Developing novel assays that utilize the latest biological advances like HiBiT is of the utmost importance for the discovery and advancement of possible therapeutics.

CHAPTER 3. GENERATION AND CHARACTERIZATION OF REPORTER HEPACIVIRUSES

3.1 Chapter Summary

In the previous chapter, HiBiT was incorporated into the structural proteins of DENV. The resulting viruses were characterized in order to assess replication, translation of viral proteins, infectivity, tag stability, and the tolerance of various other epitope tags. In this chapter, the lessons learned from the DENV model system were applied to Hepatitis C virus, another member of family *Flaviviridae*. HiBiT and other small tags were engineered within core and E2 and the resulting viruses were characterized. Various insert compositions within the N-terminus of E2 produced infectious, luminescent virus with the construct consisting of FLAG and HiBiT displaying similar peak titer as compared to WT while emitting far greater luminescence that seems to directly correlate to infectious particles. Furthermore, the FLAG and HiBiT tagged virus was capable of being purified using immunoprecipitation with anti-FLAG antibodies suggesting the tag is partially surface exposed. This multi-tagged, reporter HCV is a powerful reagent enabling quantification and purification in a more efficient and efficacious manner than the currently utilized techniques.

3.2 Introduction

Hepatitis C virus (HCV) is an important human pathogen that has infected over 170 million people worldwide (WHO, 2019). The virus attacks the liver and typically manifests in a chronic infection which can lead to cirrhosis and hepatocellular carcinoma. Despite the seriousness of chronic infection, a majority of individuals can be cured using antiviral medication that targets virus-specific proteases and other viral targets. However, a treatment regimen involving a combinatorial approach can cost upwards of \$80,000 and still may not address the emergence of resistant variants. Additionally, the lack of any prophylactic vaccine, severe side effects of existing treatments, and low response rates in cirrhotic patients all emphasize the need for new and more efficacious HCV therapeutics (Delang et al., 2013).

HCV is the sole member of the hepacivirus genus, family *Flaviviridae*, and is a positive-sense single stranded RNA virus that encodes 3 structural proteins (core, envelope-1 (E1), and

envelope-2 (E2)) and 7 nonstructural proteins (p7, NS2, NS3, NS4A, NS4B, NS5A, and NS5B). The HCV particle is comprised of a nucleocapsid core containing the viral genome and is enveloped by E1E2 heterodimers. Unlike many viruses in family *Flaviviridae*, the structure of infectious HCV is likely highly irregular because it is believed that the virus circulates as a heterogeneous lipoviral particle (LVP) (Bartenschlager et al., 2011). HCV particles have been shown to incorporate apolipoprotein E (apoE) which is known to participate in attachment and entry as well as alter the infectivity of HCV (Gong et al., 2019). The association of HCV with host lipoproteins may explain the low buoyant density for highly infectious material and the broad range of observed densities of HCV particles (1.03 to 1.25g/mL) (Catanese et al., 2013). Due to the highly pleiomorphic nature of the virus, and difficulty producing virus in cell culture, the quantification and purification of HCV remains problematic.

Despite recent advances in the production and study of HCV, there is currently no crystal structure of HCV glycoproteins or a three-dimensional reconstruction of the virion. Classical methods that have previously yielded sufficient quantities of intact *Flaviviridae* virus particles for imaging, have thus far proven inadequate for HCV (Catanese et al., 2013, Mukhopadhyay et al., 2003, Sirohi et al., 2016). Therefore, finding ways to acquire enough HCV particles for cryo-electron microscopy (cryo-EM), while saving time and resources, is of the utmost importance. One such way to aide in the quantification and subsequent purification of HCV particles is to create multi-tagged constructs that facilitate luminescent detection in tandem with well-established purification methods. However, there are several barriers that must be overcome in order to construct a viable, tagged HCV. For example, the relatively large size of conventional reporter proteins like green fluorescent protein, Renilla luciferase, or Firefly luciferase can alter the replication or infectivity of wild type virus by causing misfolding, altering dynamics, etc.

In order to overcome these issues, Promega has recently developed a split-luciferase system (HiBiT Protein Tagging System) involving a 1kDa protein (HiBiT) attached to a protein of interest that binds to a 156 amino acid, 17.6 kDa protein (LgBiT) with an affinity of 0.7 nM. After binding, the complex emits a sensitive and specific, glow-type luminescence. Thus far, researchers have been able to incorporate the HiBiT gene into NS2 of HCV with less than a half log decrease in focus forming units (FFU) (Tamura et al., 2018). Previous studies have also demonstrated HCV can tolerate small affinity tags like 6xHistidine (HIS), FLAG, and Streptavidin (Strep) (Catanese et al., 2013, Prentoe et al., 2011). The insertion of larger tags has been attempted in E2 of HCV

with moderate success, likely due to the conformational flexibility demonstrated by the protein (Kong et al., 2016). E2 is the receptor-binding protein of HCV and a common target for broadly neutralizing antibodies that has been shown, via structural studies, to exist in several different orientations when in complex with various fabs (Vasiliauskaite et al., 2017). These findings, along with existing E2-tagged constructs, support the viability of engineering HiBiT in this protein.

By incorporating both HiBiT and various purification proteins in the structural region of HCV (core, E1, E2), researchers would be able to detect and quantify HCV production via HiBiT and subsequently purify virus particles via HIS, FLAG, or Strep affinity chromatography or immunoprecipitation. Obtaining a sufficient quantity of structurally sound HCV particles has proven to be extremely difficult and any tools that aid in this aim could be very useful. In addition to structural studies, a reporter system for HCV is a powerful tool that can foster a better understanding of the viral life cycle and pathogenesis as well as assist in the development of new and more effective therapeutics.

3.3 Materials and Methods

3.3.1 Cell culture

Human hepatic (HuH-7.5) cells were cultured in Dulbecco's Modified Eagle Medium (DMEM) supplemented with 10% fetal bovine serum (FBS) with 5% CO₂ at 37°C.

3.3.2 Site directed mutagenesis

The recombinant constructs were created using site directed mutagenesis performed on full length, tagged HCV cDNA (J6/JFH1 strain) following a modified Phusion polymerase protocol (New England Biolabs, NEB). The cDNA was provided by the laboratory of Charles Rice at Rockefeller University and is a tagged clone 2 derivative encoding a duplication of amino acids 384 and 385 of the HCV polyprotein of J6, a 6x histidine repeat (HIS), and a One-STrep tag (OST) (Catanese et al., 2013). Core, E1, E2, p7, and NS2 are J6 strain derived and the remaining nonstructural proteins are JFH1 derived. Complementary, overlapping primers were designed using NEBuilder software and used for insertions and substitutions. Following the polymerase chain reaction (PCR), products were digested using *DpnI* (NEB), phosphorylated using T4 polynucleotide kinase (NEB), and ligated using T4 DNA ligase (NEB). Mutants were transformed

into DH5 α cells and plasmid DNA was extracted and checked via restriction digestion, then subsequently sequenced through either Genewiz or the Low Throughput Purdue Genomics Core Facility.

3.3.3 In vitro transcription and transfection of vRNA

Plasmid clones were linearized using XbaI enzyme and in vitro transcribed using T7 RNA polymerase (NEB) at 37°C for 1.5 hours and run on a 0.8% agarose gel to confirm RNA product size and quality. Transfection into Huh7.5 cells was performed using lipofectamine 3000 (L3000) and the protocol provided by the manufacturer (Thermo Fisher). For transfection in a 6-well plate, 2.5 micrograms of RNA for both WT and mutants were mixed in an OptiMEM (OM) solution and added to another OM solution containing L3000 at a 1:2 ratio of RNA to L3000. The mix of RNA and L3000 was added to each respective well, incubated for four hours at 37°C, and the media was replaced with DMEM supplemented with 5% FBS. Virus supernatant and lysate was harvested at 24-hour timepoints up to 120 hours post transfection (hpt) and stored at -80°C.

3.3.4 HiBiT assay

HiBiT activity was assessed using the HiBiT lytic detection kit and protocol provided by the manufacturer (Promega). Luminescence was measured with an integration time of two seconds at 470 nm in white polystyrene non-binding 96-well plates (Corning).

3.3.5 Focus unit identification assay

Approximately 10,000 Huh 7.5 cells were plated into a 96-well plate 48 hours prior to infection. 20 μ l of viral supernatant was suspended in 180 μ l DMEM supplemented with 5% FBS and 6, 10-fold dilutions were used for infection. Immediately after adding supernatant to the wells, plates were incubated at 37°C for 48 hours. The cells were then fixed with chilled methanol for 20 minutes at -20°C. Wells were then washed with PBS and a 3% solution of H₂O₂ was added to each well. After again washing with PBS, wells were blocked with bovine serum albumin (BSA) for one hour. Following blocking, fixed cells were probed with an anti-NS5 antibody (Rice Lab) at a dilution of 1:2000 and rocked overnight at 4°C. Goat anti-Mouse conjugated HRP (Abcam) was added to each well at a dilution of 1:500 and rocked at room temperature for 1 hour. Each

well was extensively washed with PBS and 60µl of TrueBlue substrate (SeraCare) was added to each well.

3.3.6 Immunofluorescence assay

Huh 7.5 cells were plated into a 24-well plate approximately 24 hours prior to infection. Transfected cell supernatant (500µl) collected at the appropriate timepoints was added to the wells, rocked for two hours at room temperature, and each well's media was replaced with fresh DMEM supplemented with 2% FBS. The infection proceeded for 48 hours at 37°C. The cells were then fixed with chilled methanol for 20 minutes at -20°C. Wells were then washed with PBS and blocked with BSA for one hour. Following blocking, fixed cells were probed with an anti-NS5 antibody (provided by the laboratory of Charles Rice at Rockefeller University) at a dilution of 1:2000 and rocked overnight at 4°C. FITC secondary antibody (Abcam) was then added at a dilution of 1:500 and rocked at room temperature for 1 hour. Nuclei were counterstained with propidium iodide and cells were visualized using fluorescent microscopy.

3.3.7 SDS-PAGE and western blot

Transfected or infected cell supernatant and lysate were collected at 24-hour time points. Cells were lysed through the addition of 250µl of RIPA buffer. SDS-PAGE was performed using a 10% acrylamide gel with or without heating samples for 5 minutes at 95°C depending on the protein being visualized. Additionally, samples were mixed with loading dye and BME depending on whether reducing conditions were necessary. The nitrocellulose membrane was probed with anti-FLAG or anti-NS5 antibodies. Secondary antibodies with infrared-labels (680-800nm) were added to the membrane and visualization was done utilizing an Odyssey infrared imager (Li-COR).

3.3.8 FLAG affinity purification

Immunoprecipitation was performed using the FLAG immunoprecipitation kit (Sigma-Aldrich). Transfected cell supernatant from the 96 hpt timepoint was filtered using a 100kDa filter and one ml was used for downstream procedures. 50µl of Anti-FLAG M2-Agarose Affinity Gel was thoroughly washed with 1x wash buffer and once with elution buffer. Sample was added to the affinity beads and rotated at 4 °C overnight. Sample was then thoroughly washed and

resuspended in FLAG peptide at a concentration of 150µg/ml. 100µl of initial sample, flow through, and each respective wash following flow through were saved and used for HiBiT assay analysis.

3.4 Results

3.4.1 Determination of insert loci and construct variation

Due to no available structure of the reconstructed HCV particle, prior research was analyzed to determine additional locations for HiBiT insertion within the N-terminal E2 site. Previous studies were also reviewed for possible sites within core protein. Researchers have been able to engineer the tetracysteine (TC) tag, an epitope typically used for fluorescent labeling, within the N-terminus of core protein with only approximately a log decrease in infectious titer (Coller et al., 2012). TC is six amino acids which is comparable to HiBiT in size. Additionally, engineering HiBiT within the core of HCV would enable researchers to differentiate HCV infectious particles from subviral particles (SVPs). Although such a tool would be very useful, the tag would not be surface exposed and, therefore, would not be useful for purification purposes. E2 of HCV has been extensively studied and shown to be very flexible which indicates the possibility of incorporating the HiBiT epitope in this protein with little influence on fitness.

E2 is the receptor binding protein of HCV and a common target for neutralizing antibodies. Multiple conformations when bound to Fabs have been observed, suggesting the flexibility necessary for tagging (Ströh et al., 2018). Researchers have also incorporated several different tags of varying size into the N-terminus of E2 including OST, FLAG, and HIS, among others (Catanese et al., 2013, Prentoe et al., 2011). Three variations of the OST-tagged plasmid, provided by the Rice lab, were constructed that each contained a repeat of amino acids (aa) 384-385 to conserve cleavage. One construct contained only HiBiT because incorporating tags of a similar size compared to HiBiT, like FLAG, have had little to no impact on fitness. The other construct consisted of both FLAG and HiBiT in order to potentially serve both quantification and purification purposes. Finally, the OST plasmid was modified to contain a HIS tag, the HiBiT gene, and one StrepII tag with appropriate spacers. Since the OST recombinant virus had been shown to only decrease viral titer by one log, this construct was created in order to maintain a similar size as compared to the OST insert while adding quantification capacity through the use of

HiBiT (Catanese et al., 2013). Although the OST tag has been shown to enhance affinity to streptavidin beads as compared to a single StrepII tag, conserving size of the insert was deemed more important than a possible increase in affinity (Catanese et al., 2013). Each of the four constructs, in addition to a WT construct consisting of a deletion of the OST and repeated aa, were engineered using the previously described SDM methodology and characterized alongside the OST virus (Figure 3.1, Table 3.1).

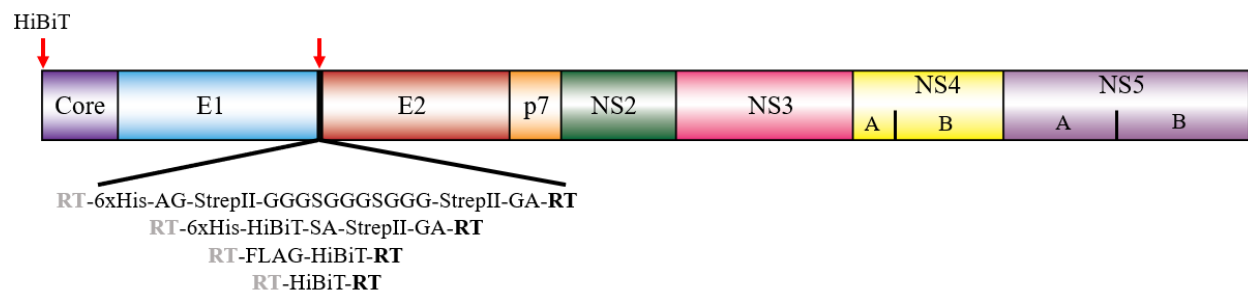


Figure 3.1 Insert loci and composition within HCV genome. A schematic representation of HCV and the location of engineered inserts. Red arrows indicate tag insertion sites and composition of the inserts are described above the schematic for the core site while the N-terminal E2 site is described below the schematic. The amino acids in bold represent the cleavage site for E1/E2 with gray font representing the wild type amino acids which were repeated in the construct in order to ensure proper cleavage.

Table 3.1 HCV-HiBiT tag locations and construct variation. Table describing tag locations with viral protein, protein region, preceding amino acid within viral protein, nucleotide in full length genome, and tag composition specified.

Protein	Protein Region	Amino Acid in Protein	Nucleotide in Genome	Tag Composition
Core	N-terminus	3	439	HiBiT
		2	1495	6xHIS-AG-StrepII-2(GGGS)GGG-StrepII-GA-RT
E2	N-Terminus	2	1495	6xHIS-HiBiT-SA-StrepII-GA-RT
		2	1495	FLAG-HiBiT-RT
		2	1495	HiBiT-RT

3.4.2 Initial characterization of recombinant HCV replication and translation

After constructing cDNA clones of each construct, the plasmids were *in vitro* transcribed and transfected into Huh 7.5 cells. The supernatants of transfected cells were collected at 24-hour

timepoints and a HiBiT assay was performed on each respective clone. HiBiT activity from 24 to 96 hpt revealed that the HiBiT-Core recombinant virus had little to no replication with only a slight growth in activity from 24 to 48 hpt, peaking at a signal of 3×10^3 RLU. All other tagged virus demonstrated a significant increase in HiBiT activity as compared to WT (Figure 3.2). Notably, the FLAG-HiBiT-E2 virus emitted the highest HiBiT signal with a peak value of 1×10^8 RLU at 96 hpt. Both HIS-HiBiT-Strep-E2 and HiBiT-E2 displayed similar replication kinetics and peaked slightly above 10^6 RLU. In order to initially assess infectivity, transfected cell supernatants were used to infect naïve Huh 7.5 cells for immunofluorescence assay (IFA).

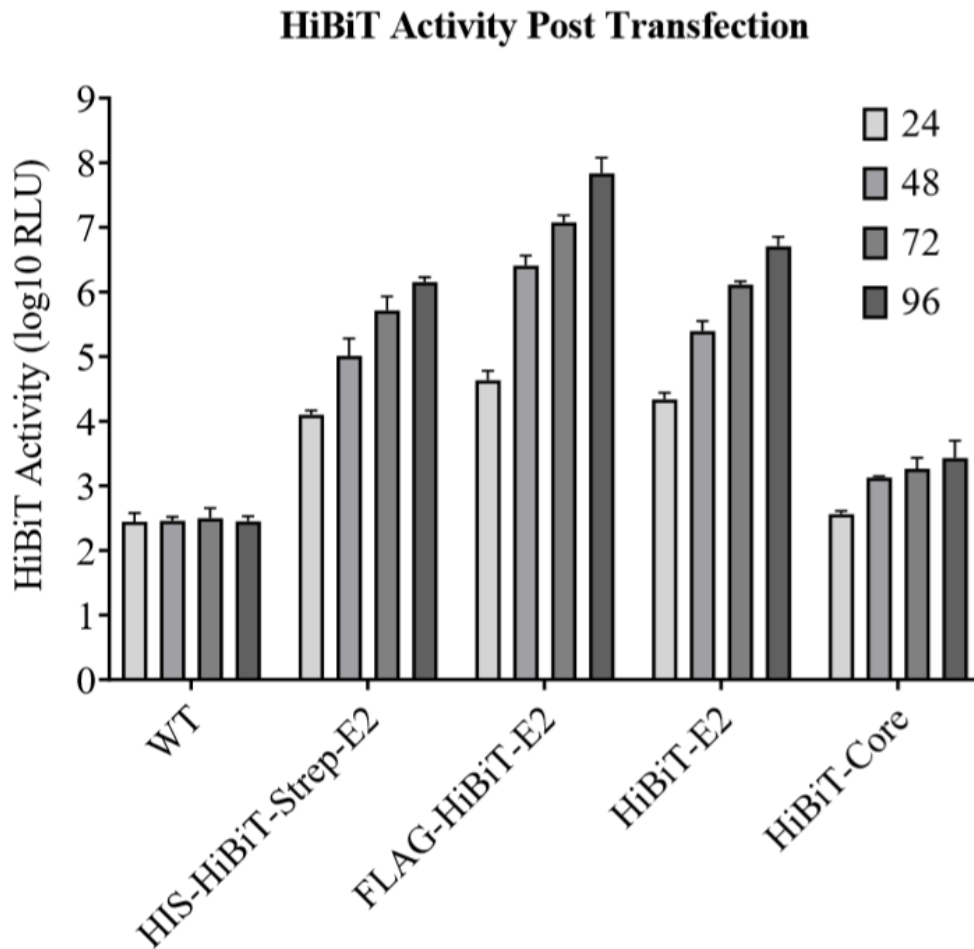


Figure 3.2 Luminescence of transfected cells at 24 to 96 hours post transfection. Viral HCV RNA was transfected in Huh 7.5 cells via L3000 and seeded in a 6-well plate format. At 24-hour timepoints post transfection, 100 μ l of the supernatant was lysed with the HiBiT lytic reagent and luminescence was measured with an integration time of two seconds at 470 nm. The remaining supernatant was collected and stored at -80°C. Luminescence is measured in relative light units.

3.4.3 Characterization of recombinant HCV infectivity

The HiBiT activity post transfection revealed that the peak titer would likely occur at 96 hpt (Figure 3.2) and, therefore, 500 μ l of the 96 hpt supernatant for each clone was used to infect one well of a 24-well plate seeded 24 hours prior to infection. The infection proceeded for 48 hours after which the cells were fixed, probed with anti-NS5 antibodies, FITC secondary antibodies, and counterstained with PI (Performed by Devika Sirohi). As anticipated, the HiBiT-Core virus appeared to produce no infectious particles. All other recombinant viruses were capable of first round infection as demonstrated by the overlay of FITC and PI signal. The OST-E2, FLAG-HiBiT-E2, and HiBiT-E2, all appeared to demonstrate similar infectivity with nearly all of the cells in the visual field infected (Figure 3.3). In order to more quantitatively assess infectious titer, all samples were processed using HiBiT and FFU assay of 96 hpt supernatant.

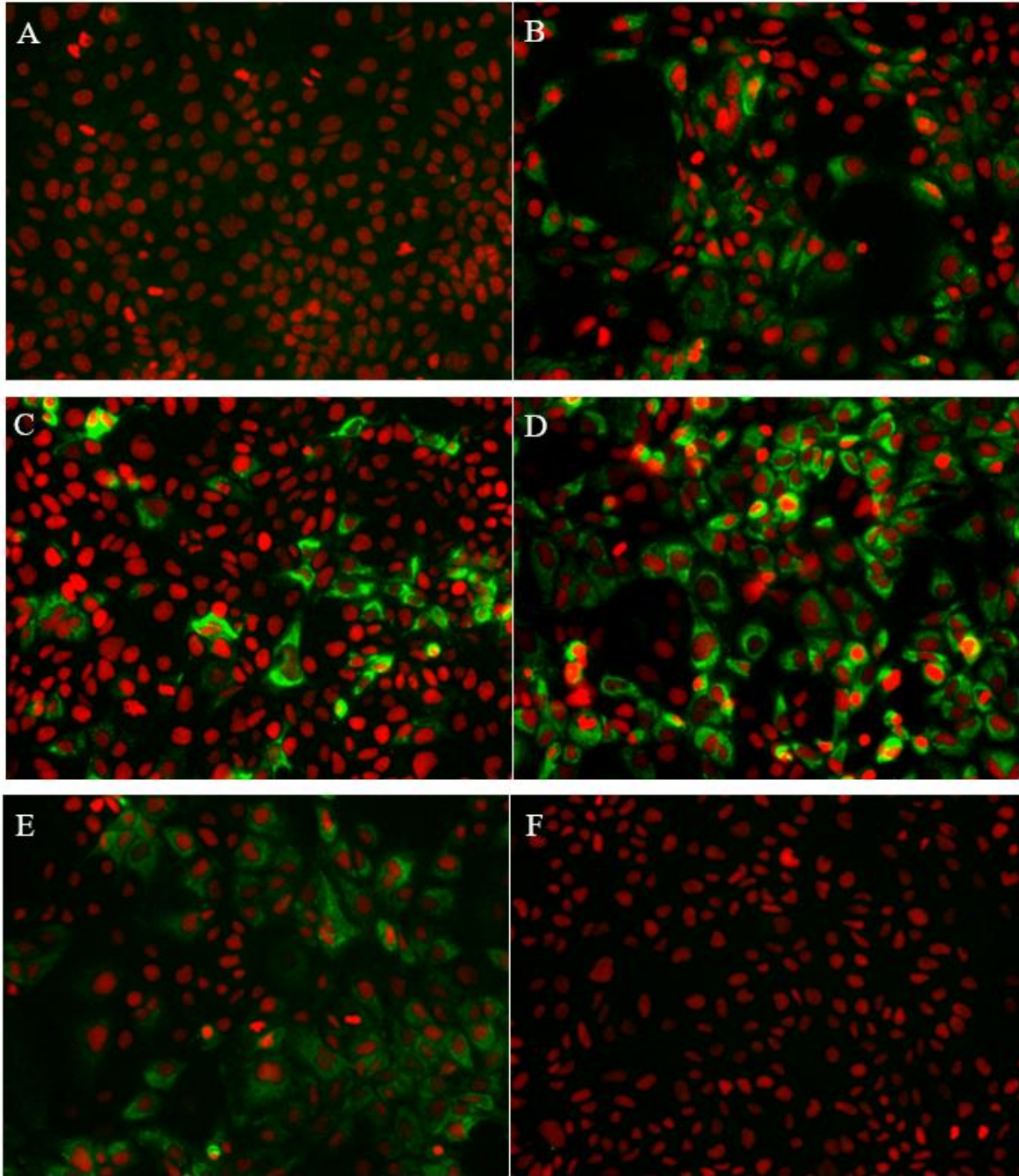


Figure 3.3 Infectivity of recombinant virus assessed by immunofluorescence. Huh7.5 cells were seeded in a 24-well plate and incubated until 90-100% confluency was reached. 500 μ l of supernatant collected at 96 hpt was added to each respective well and the plate was rocked for 2 hours at room temperature. Infection proceeded for 48 hours at which point the plates were fixed with methanol, blocked with BSA, and probed with anti-NS5 antibodies, FITC secondary antibodies, and counterstained with PI. (A) mock, (B) OST-E2, (C) HIS-HiBiT-StrepII-E2, (D) FLAG-HiBiT-E2, (E) HiBiT-E2, (F) HiBiT-Core.

The transfected cell supernatant collected at the 96 hpt timepoint was further assessed with HiBiT assay and 6, 10-fold serial dilutions were used to infect naïve Huh 7.5 cells for FFU. The FLAG-HiBiT-E2 virus yielded the highest titer of the recombinant viruses with approximately 8.3×10^5 FFU/ml which corresponded to a HiBiT value of 8.03×10^7 RLU (Figure 3.4). This compares to a WT titer of 1.3×10^6 FFU/ml and a HiBiT value of 3.1×10^2 RLU. The construct provided by the Rice lab yielded virus with a peak titer slightly lower than the FLAG-HiBiT-E2 at 3.3×10^5 FFU/ml and HiBiT value similar to that of WT infected cells. As expected, the HiBiT-Core construct produced no infectious particles but still produced a HiBiT value above that of WT at 10^3 RLU, which may simply be a remnant of initial transfected RNA and resulting translation. HIS-HiBiT-Strep-E2 and HiBiT-E2 demonstrated a titer approximately three and two logs lower than that of WT and produced HiBiT activity values corresponding to their titer at 1.2×10^6 and 7.3×10^6 respectively. Following initial titration of the recombinant viruses, the FLAG-HiBiT-E2 and OST-E2 were chosen for further characterization and the growth kinetics of each virus were assessed.

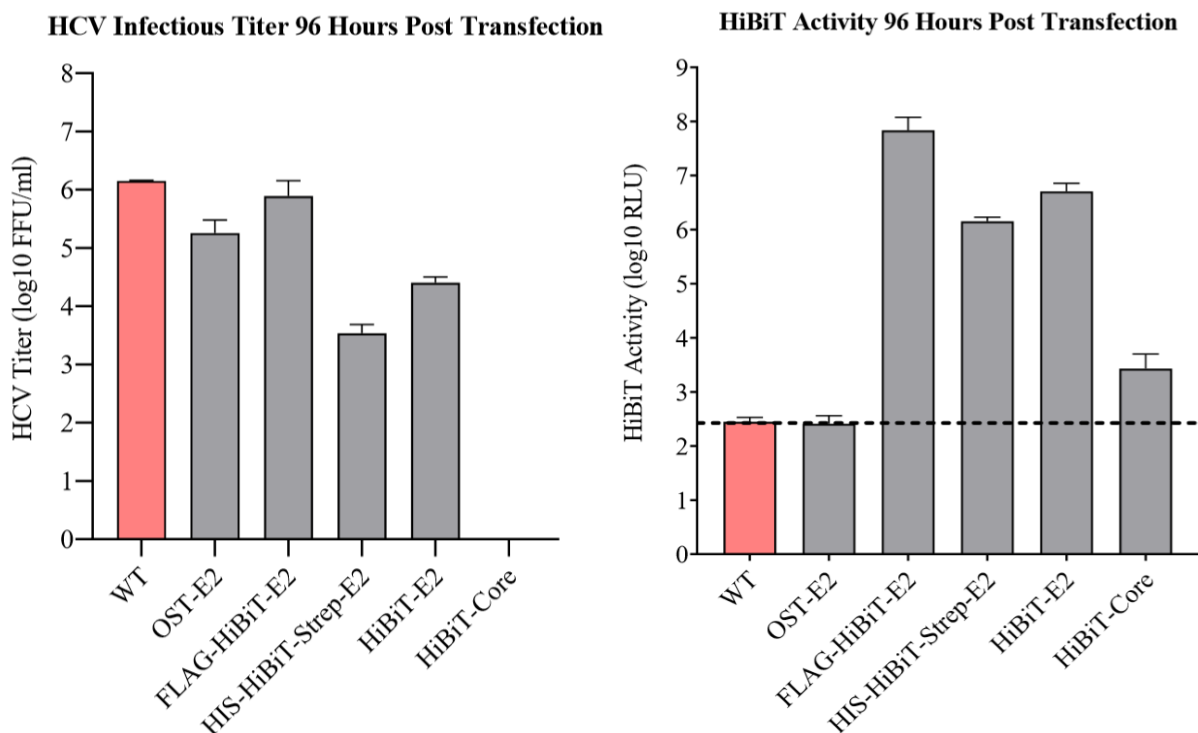


Figure 3.4 Peak titer and HiBiT activity for recombinant HCV. Viral HCV RNA was transfected in Huh 7.5 cells via L3000 and seeded in a 6-well plate format. At 96 hours post transfection, 100 μ l of the supernatant was lysed with the HiBiT lytic reagent and luminescence was measured with an integration time of two seconds at 470 nm (Right). Infectious titer of the supernatant was then assessed via FFU assay (Left).

3.4.4 FLAG Immunoprecipitation

Following the characterization of the FLAG-HiBiT-E2 virus infectivity and growth pattern, the virus was subjected to immunoprecipitation with antibodies targeting the FLAG peptide. Transfected cell supernatant collected at the 96 hpt timepoint was spun down and purified using a 100 kDa filter. Purified supernatant was incubated with beads coated in anti-FLAG antibodies and eluted in a solution containing FLAG peptide. The HiBiT activity was assessed for the input, flow through, each wash following flow through, and the final elution. Total RLU per volume assessed was calculated and compared to the input as a percentage. According to the HiBiT data analyzed, FLAG immunoprecipitation with FLAG-HiBiT-E2 results in 25.97% of the total input RLU being detected in the final elution (Figure 3.5). Flow through accounted for another 25.5% of the total input RLU with each following wash resulting in smaller percentages of total RLU. Each sample was diluted in wash buffer at a 1:10 ratio to ensure the media did not interfere with HiBiT signal.

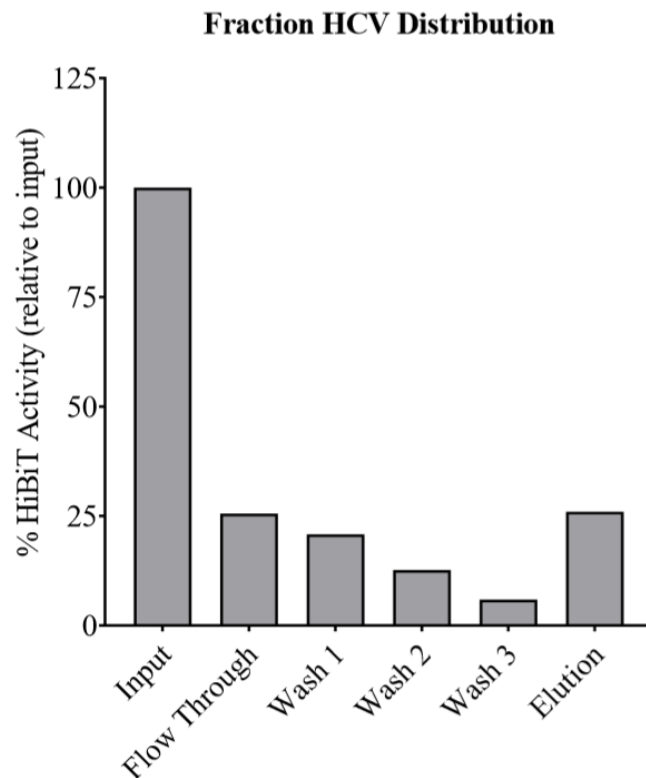


Figure 3.5 FLAG immunoprecipitation with efficiency determined by HiBiT activity. 100 kDa filter-purified infected cell supernatant was immunoprecipitated using the Anti-FLAG M2 affinity kit. Approximately 100 μ l of sample from each step was stored for HiBiT assay. 10 μ l of each sample was suspended in 90 μ l of wash buffer and HiBiT activity was assessed. Using the HiBiT signal from the 10 μ L sample, total RLU per volume of total sample was calculated and the input RLU was used as 100%.

3.5 Discussion

HCV is a highly pleiomorphic and lipophilic virus which has made structural studies particularly difficult. In order for a tagged virus to be used to aide researchers in preparation for cryo-EM, the recombinant virus must behave as closely to WT as possible. Any decrease in titer or delay in growth kinetics entails a significant burden for those tasked with preparing the large quantities of virus necessary for visualization. Previous studies have characterized a tag site within the N-terminus of E2 and shown that inserts in this location have little effect on fitness (Catanese, et al., 2013). This virus was characterized further within this study and other tag variations were inserted at this location in the genome. Additionally, one tag site was attempted within core protein. The characterization of these recombinant viruses revealed several possible reporter viruses which

could be used for both virus quantification and purification, saving researchers time and money throughout the course of HCV structural studies.

Initial characterization revealed the FLAG-HiBiT-E2 virus as a top candidate for further analysis. This virus displayed the highest peak titer and luminescent signal following transfection, with HiBiT-E2 and HIS-HiBiT-Strep-E2 displaying slightly lower peak titer and luminescence (Figure 3.2). The HiBiT-Core virus appeared to have a replication defect because the amount of HiBiT signal remained stagnant for all timepoints post transfection. However, all others demonstrated a steady increase in HiBiT signal post transfection, indicating replication and translation competence as well as suggesting possible first and second round infection. All recombinant viruses were subjected to IFA screening and each were found to infect naïve Huh7.5 cells at varying efficiency, apart from HiBiT-Core (Figure 3.3). Once again, IFA results seemed to indicate FLAG-HiBiT-E2 as the recombinant virus with the highest titer and this notion was confirmed with the FFU assay showing the virus had an infectious titer nearly identical to WT (Figure 3.4). The OST-E2 virus displayed similar characteristics described by previous studies, to include approximately a log decrease in WT infectious titer (Catanese et al., 2013).

There are several possible reasons for inhibition of infectious titer for the HIS-HiBiT-Strep-E2 and HiBiT-E2 viruses. Although there were appropriate spacers for the StrepII tag, additional flexible linkers were not added for the other tags which may have resulted in a disruption of the envelope proteins of HCV and their ability to bind to apoE or other lipoproteins. Additionally, the composition of the insert could have adversely affected replication or any number of steps in the HCV life cycle as was demonstrated with DENV in chapter 2 of this study. HiBiT-E2 virus produced less virus as compared to the FLAG-HiBiT-E2 virus which could be due to variation in composition of the two tags. Perhaps, due to the lack of structure and negative charge of FLAG, the FLAG epitope served as a spacer for the HiBiT tag and added additional flexibility. Regardless of the reasons for differences in titer of tagged virus, the E2 site proved to be a region susceptible to tagging.

This site within E2 is likely able to tolerate insertions due to its hypervariability and well characterized conformational flexibility (Law et al., 2018). The hypervariable region of E2 consists of the first 27 aa and is known to play a role in the evasion of neutralizing antibodies by shielding certain epitopes in a dynamic manner. Results in this study seem to confirm that this region can tolerate relatively large insertions with virtually no effect on replication or infectivity.

E2 functions as a sort of “flap” that has been visualized in several different conformations when bound to Fabs, suggesting there is a high degree of flexibility which allows for tagging without additional steric hindrance (Vasiliauskaite et al., 2017). Furthermore, due to the use of the HiBiT lytic detection system, the surface exposure of HiBiT in the native state did not impact HiBiT-LgBiT binding and, therefore, the virus was able to be quantified using HiBiT signal. However, in order for this virus to be purified for structural studies, the FLAG epitope must not only be tolerated but also surface exposed.

FLAG immunoprecipitation with FLAG-HiBiT-E2 infected supernatant revealed that the FLAG tag is likely partially surface exposed as approximately 26% of virus particles were rescued (Figure 3.5). Loss of virus during the washes indicates some nonspecific binding which has been shown to occur with the Anti-FLAG affinity kit utilized. Previous reports have shown that FLAG purification using a FLAG peptide inserted in this region of E2 recovered approximately 30% of particles, which aligns well with the findings in this study (Prentoe et al., 2011). Insertion of the FLAG peptide seems to have not altered the physiochemical properties of the virion and therefore the tagged virus can be used for imaging purposes, composition analysis, and other downstream assays. There are very few commercially available antibodies for E2 and, thus, a FLAG peptide in this region could prove a valuable tool for western blots, ELISA assays, and more.

With the advancement of imaging techniques such as cryo-EM and cryo-ET, structural studies of complex viruses are within reach for the first time in modern history. However, reconstruction of the HCV particle has proven challenging, and attempts at solving the structure have had little success. The virus characterized in this study enables large scale purifications with greater ease than before. High concentrations of intact particles must be properly isolated in order to ascertain a high-resolution image. Using the HiBiT tag to quantify HCV particles is a quick, cost-effective method of ensuring the efficacy of every step of virus propagation and the FLAG tag provides a method for highly specific immunoprecipitation. The HiBiT and FLAG tagged HCV in this study is a powerful reagent that may prove very useful in HCV study and, eventually, the development of cheaper therapeutics and a viable vaccine.

CHAPTER 4. CONCLUSIONS AND FUTURE DIRECTIONS

The *Flaviviridae* family of viruses includes many important pathogens like DENV and HCV that infect millions of people each year. In order to produce new and effective therapeutics for these pathogens, *Flaviviridae* virus structures and life cycles must be better understood. The development of novel, and relatively small, reporter proteins like HiBiT has enabled more targeted studies that were otherwise impossible with larger, conventional reporter proteins like GFP. This study served to construct and characterize recombinant reporter viruses containing the HiBiT gene to be used as quantifiable reagents for downstream assays. The initial objectives of this research were two-fold: to use HiBiT as a means of quantifying flaviviruses and to use the positioning of HiBiT within flavivirus structural proteins to assess HiBiT-LgBiT binding and, thus, the accessibility of the tagged region. After initial characterization of DENV tagged clones, the research presented new questions to be explored such as the importance of tag composition, length, and position within the viral protein. The lessons learned through analyzing recombinant DENV containing the HiBiT gene were then applied to HCV with the objective of constructing and characterizing a multi-tagged reporter virus containing both HiBiT and a purification tag to enable more efficient preparation of samples for structural studies. The luminescent activity and infectious titer stability of assessed mutants confirm the viability of HiBiT reporter viruses as powerful tools to investigate virus production and structure.

Initial construction and characterization of recombinant DENV containing the HiBiT gene centered around establishing a positive control tagged DENV to use as baseline luminescence for comparison against tag sites explored in this study. Previous findings demonstrated the ability of flaviviruses to tolerate reporter genes within NS1 and, thus, several sites within DENV NS1 were attempted. HiBiT inserted into both the N and C terminus of NS1 yielded virus with a decrease of three and two logs, respectively, which was deemed too low of titer to be used as a control for structurally tagged recombinant virus. However, many studies have found NS1 to be a protein of high plasticity within the flavivirus genome (Eyre et al., 2017, Tamura et al., 2018, Tamura et al., 2019). In fact, the N-terminus of NS1 in DENV has been found to tolerate APEX, an EM tag with a size of 27 kDa, with only approximately a log decrease in viral titer. With slight adjustments to the construct variation compared to what was attempted in this study, the NS1-HiBiT recombinant virus may very well achieve near WT titer.

If a viable NS1-HiBiT reporter virus was constructed, it could prove to be a useful tool for *in vitro* as well as *in vivo* studies. NS1 is an enigmatic protein that serves many different functions in the flavivirus life cycle and is even secreted as a hexamer following maturation via glycosylation. NS1 is also typically used as a diagnostic marker for flaviviruses and has been found to play a role in immune evasion as well as modulate the host response to infection (Ratsogi, 2016). The findings in this study, as well as previous research, suggest that a HiBiT tagged NS1 could function to track the viral protein throughout the viral life cycle and possibly be used as a platform to develop novel therapeutics. Serial passaging and qRT PCR of the recombinant virus characterized in this study should be performed to characterize the replication competence and stability of the insert. Furthermore, additional construct variations to include various linker orientations and location within the genome should be attempted and characterized.

Although the construction of a HiBiT flavivirus positive control did not yield WT level titer, the findings strongly suggested the possibility of tagging flaviviruses with HiBiT. After the HiBiT screening methodology, described in chapter two, and titration via plaque assay was completed, two clones were found to tolerate HiBiT insertion and produce infectious virus. The recombinant virus with HiBiT inserted after aa 103 in C protein is a particularly interesting mutant because of the HiBiT location being after the first three aa (SAG) of helix $\alpha 5$, the C propeptide. This anchor peptide recruits a signal peptidase for cleavage from prM and NS2B/NS3 for cleavage at the $\alpha 4/\alpha 5$ helix junction. Previously it has been thought that, following cleavage, the helix remains embedded in the ER membrane and only the mature, cleaved C protein is involved in flavivirus assembly. All previous structures of flavivirus C protein reflect this notion (Ma et al., 2004, Li et al., 2018). However, the findings in this study confirm new structural analyses indicating that mature, cleaved capsid is likely incorporated into flavivirus particles along with uncleaved capsid containing helix $\alpha 5$ (Tan et al, 2020).

The C-103 recombinant virus was found to be stable over three passages in BHK cells and maintained a similar luminescent signal throughout. Furthermore, isolated virus particles were found to correspond with peak HiBiT signal. However, this HiBiT signal may not correlate with the 180 copies of capsid expected in the mature flavivirus particle. Tan et al. found that capsid exists within the particle as a heterogeneous population of both cleaved and uncleaved, with the exact ratio between the two unknown. The findings in this study seem to indicate that HiBiT does not completely inhibit the hypothesized role of helix $\alpha 5$ in assembly. Furthermore, the tag does

not seem to disturb NS2B/NS3 signal peptidase cleavage at the helix junction. In order to further confirm this notion, a western blot with a C protein antibody could be performed to assess the proportion of cleaved vs uncleaved capsid in the supernatant. HiBiT antibodies could be used to probe whether the tag colocalizes with C protein which would further support the findings stated above. As is, the C-103 recombinant virus could be used for several purposes including a nucleocapsid incorporation assay which has been performed using pulse-chase methodology in the past (Setoh et al., 2015). Although the HiBiT signal would not directly correlate with each C protein monomer, the signal would indicate the presence of helix $\alpha 5$ within the virus particle. Another purpose of the C-103 HiBiT mutant could be assessment of signal peptidase cleavage at the C-prM junction. Due to the necessity of sequential cleavage, first at the $\alpha 4/\alpha 5$ junction followed by C-prM, mutations at the C-terminus of the propeptide could be more efficiently analyzed (Amberg et al., 1999). The findings in this study indicate that NS2B/NS3 cleavage is minimally affected by HiBiT insertion. Therefore, HiBiT signal could be used as a medium of comparison between C-terminus mutants and the C-103 virus. Following additional characterization of C-103 recombinant virus behavior, it could prove a useful reagent to gain further insight into the mysterious signal peptide and its role in the flavivirus life cycle.

Other findings from the flavivirus portion of this study include the limited tolerance of HiBiT within the M protein transmembrane domain and the importance of tag composition within EDI. Reasons for the loss of HiBiT signal over the course of serial passaging the M-55 virus were discussed in chapter two but it is likely that the tag was excised due to the importance of prM/M interactions with C protein at this site. According to structural fittings of C protein densities, the region where HiBiT tag is incorporated in the M-55 mutant may be critical for assembly (Tan et al., 2020, Therkelsen et al., 2018). The HiBiT tag likely disrupted important interactions between the transmembrane domain of M and C protein resulting in reversion, explaining the rescue of WT titer. Similarly, incorporating HiBiT at site E-149 inhibited the production of infectious particles.

The sites attempted within EDI in this study were near one of the glycosylation sites of DENV as well as the fusion loop of the adjacent E protein monomer. Without solving the structure of the tagged virus, it is unknown how exactly HiBiT is displayed on the glycoprotein but due to the recombinant virus' inability to produce infectious particles, it likely disrupts either glycosylation or fusion. The EDI tag sites yielded some of the highest luminescent signals post electroporation (Figure 2.3), which possibly suggests that particles are being produced but are

inhibited during first round infection. An entry assay should be completed with the supernatant from transfected cells to assess whether the virus is entry deficient or whether the virus can enter new cells but remains in the endosome. However, incorporation of the FLAG epitope and SmBiT in site E-149 was able to rescue varying degrees of infectivity. Due to no available structure of SmBiT, it is tough to determine exactly why HiBiT completely inhibits infectivity but SmBiT does not. FLAG-tagged virus at site E-149 experienced only a log decrease in infectious titer which was expected according to previous studies (Chambers et al., 2018). Proper protein folding and structure of EDI was likely not affected due to the lack of structure of FLAG. If the product of the HiBiT-tagged DENV at site E-149 is stable, and enough supernatant is collected and purified, structural studies to include negative stain EM should be completed to assess how HiBiT insertion affects the structure of E protein.

After optimizing the cloning methodology and execution of HiBiT related assays with DENV, tagging was attempted with HCV. E2 of HCV contains a hypervariable region within its N-terminus known for conformational flexibility. Several tags have been incorporated in this site including a One-STrep tag, a construct that was provided to the lab by the Rice Lab at the Rockefeller University. This tagged virus had been shown to only experience a one log decrease in WT titer and displayed similar physiochemical characteristics to the WT virus. Variants of the construct were created and the virus containing both FLAG and HiBiT tags in the E2 site demonstrated nearly identical titer as compared to WT. Immediate next steps for this recombinant virus would be to characterize the growth kinetics by infecting naïve Huh 7.5 cells and titrating various timepoints to assess the rate of release. Assuming the growth curve is similar for FLAG-HiBiT-E2 and WT, this virus could prove particularly useful for the preparation of large quantities of virus particles. Aside from the preparation for structural studies discussed in chapter three, dynamics studies may be possible as well. The hypervariable region of E2 seems to experience significant dynamic motion over the course of the life cycle and E2 binds to lipoproteins at varying rates (Bartenschlager et al., 2011, Prentoe et al., 2011). Utilizing the extracellular detection kit (Promega), intact particles could be incubated with LgBiT in various conditions. Differential luminescent signal would indicate differential accessibility of HiBiT due to binding of the two components being necessary for luminescence. Different temperatures, pHs, incubation times, and many other conditions could be tested to see how HiBiT binding is affected. Density analysis with

the HiBiT tagged virus could also be completed to see how lipoprotein binding affects HiBiT signal and whether this particular site is occluded, and to what extent.

The FLAG-HiBiT-E2 virus was then used for FLAG immunoprecipitation and approximately 26% of virus particles were rescued using anti-FLAG coated beads, which aligns with previous findings of FLAG-tagged HCV purified utilizing the FLAG peptide (Prentoe et al., 2013). Other methods such as purification using heparan sulfate have been attempted with HCV but utilizing the FLAG-tagged virus characterized in this study ensures only virus particles incorporating E2 are purified. This may prove particularly important considering the necessity of highly purified samples for structural studies. Aside from virus purification, a FLAG-tagged HCV may prove very valuable for confocal imaging and colocalization studies. Previous studies have demonstrated nearly 90% neutralization with antibodies against the flag peptide in this site (Prentoe et al., 2013). This finding further suggests that steric hindrance in this region can have a dramatic effect on virus infectivity and explains why other, bulkier, tag constructs did not produce infectious virus in this study.

The original goal of this portion of the study was to make the process of virus purification more efficient in order to aid in solving the structure of HCV. Therefore, the future directions for the FLAG-HiBiT-E2 mutant are to use this virus for visualization via cryo-EM or cryo-ET. Large volumes of the sample can be prepared via electroporation or first round infection. Following transfection or infection, the virus can be concentrated using FLAG immunoprecipitation in conjunction with filtration. Using HiBiT signal as an indication of the sample concentration, researchers can repeat purification until the virus sample meets the requirements for cryo-EM. Ideally, the method described above will yield sufficient particles for a high-resolution reconstruction of HCV and possibly even the HiBiT tag.

Family *Flaviviridae* contains important human pathogens, many of which have few treatment options and no available vaccine. In order to work towards developing these therapeutics, a better understanding is needed of the life cycle of these viruses, the complex conformational changes that occur throughout the life cycle, and the structural features that make those changes possible. New and innovative biomolecular tools are being developed that enable the investigation of these processes. The incorporation of HiBiT and other tags into DENV and HCV in this study serves not only to develop reagents to further research, but also to use the incorporated tags in a manner that illuminates previously unaddressed research questions.

REFERENCES

- Alazard-Dany, N., Denolly, S., Boson, B., & Cosset, F. L. (2019). Overview of HCV Life Cycle with a Special Focus on Current and Possible Future Antiviral Targets. *Viruses*, *11*(1), 30. doi:10.3390/v11010030
- Amberg, S. M., Nestorowicz, A., McCourt, D. W., & Rice, C. M. (1994). NS2B-3 proteinase-mediated processing in the yellow fever virus structural region: in vitro and in vivo studies. *Journal of virology*, *68*(6), 3794–3802.
- Amberg, S. M., & Rice, C. M. (1999). Mutagenesis of the NS2B-NS3-mediated cleavage site in the flavivirus capsid protein demonstrates a requirement for coordinated processing. *Journal of virology*, *73*(10), 8083–8094.
- Apte-Sengupta, S., Sirohi, D., & Kuhn, R. J. (2014). Coupling of replication and assembly in flaviviruses. *Current opinion in virology*, *9*, 134–142. <https://doi.org/10.1016/j.coviro.2014.09.020>
- Bartenschlager, R., Penin, F., Lohmann, V., & André, P. (2011). Assembly of infectious hepatitis C virus particles. *Trends in Microbiology*. Elsevier Ltd. <https://doi.org/10.1016/j.tim.2010.11.005>
- Beasley, D. W., Whiteman, M. C., Zhang, S., Huang, C. Y., Schneider, B. S., Smith, D. R., ... Barrett, A. D. (2005). Envelope protein glycosylation status influences mouse neuroinvasion phenotype of genetic lineage 1 West Nile virus strains. *Journal of virology*, *79*(13), 8339–8347. doi:10.1128/JVI.79.13.8339-8347.2005
- Brady, O. J., Gething, P. W., Bhatt, S., Messina, J. P., Brownstein, J. S., Hoen, A. G., ... Hay, S. I. (2012). Refining the global spatial limits of dengue virus transmission by evidence-based consensus. *PLoS neglected tropical diseases*, *6*(8), e1760. doi:10.1371/journal.pntd.0001760
- Campbell, R. E., Tour, O., Palmer, A. E., Steinbach, P. A., Baird, G. S., Zacharias, D. A., & Tsien, R. Y. (2002). A monomeric red fluorescent protein. *Proceedings of the National Academy of Sciences of the United States of America*, *99*(12), 7877–7882. doi:10.1073/pnas.082243699
- Castelli, M., Clementi, N., Pfaff, J. *et al.* (2017). A Biologically-validated HCV E1E2 Heterodimer Structural Model. *Sci Rep* **7**, 214 doi:10.1038/s41598-017-00320-7
- Catanese, M. T., Uryu, K., Kopp, M., Edwards, T. J., Andrus, L., Rice, W. J., ... Rice, C. M. (2013). Ultrastructural analysis of hepatitis C virus particles. *Proceedings of the National Academy of Sciences of the United States of America*, *110*(23), 9505–9510. doi:10.1073/pnas.1307527110
- Chalfie M, Tu Y, Euskirchen G, Ward WW, Prasher DC. (1994). Green fluorescent protein as a marker for gene expression. *Science* *263*:802–805. doi:10.1126/science.8303295

- Chambers, M. T., Schwarz, M. C., Sourisseau, M., Gray, E. S., & Evans, M. J. (2018). Probing Zika Virus Neutralization Determinants with Glycoprotein Mutants Bearing Linear Epitope Insertions. *Journal of virology*, 92(18), e00505-18. doi:10.1128/JVI.00505-18
- Chatel-Chaix, L., Baril, M., & Lamarre, D. (2010). Hepatitis C Virus NS3/4A Protease Inhibitors: A Light at the End of the Tunnel. *Viruses*, 2(8), 1752–1765. doi:10.3390/v2081752
- Chen, X., Zaro, J. L., & Shen, W. C. (2013). Fusion protein linkers: property, design and functionality. *Advanced drug delivery reviews*, 65(10), 1357–1369. doi:10.1016/j.addr.2012.09.039
- Chevaliez S, Pawlotsky JM. HCV Genome and Life Cycle. In: Tan SL, editor. Hepatitis C Viruses: Genomes and Molecular Biology. Norfolk (UK): Horizon Bioscience; 2006. Chapter 1.
- Coller, K. E., Heaton, N. S., Berger, K. L., Cooper, J. D., Saunders, J. L., & Randall, G. (2012). Molecular determinants and dynamics of hepatitis C virus secretion. *PLoS pathogens*, 8(1), e1002466. <https://doi.org/10.1371/journal.ppat.1002466>
- Delang L, et al. (2013). Hepatitis C virus-specific directly acting antiviral drugs. *Curr Top Microbiol Immunol*. 369:289–320.
- Dixon AS, Schwinn MK, Hall MP, Zimmerman K, Otto P, Lubben TH, Butler BL, Binkowski BF, Machleidt T, Kirkland TA, Wood MG, Eggers CT, Encell LP, Wood KV. (2016). NanoLuc complementation reporter optimized for accurate measurement of protein interactions in cells. *ACS Chem Biol* 11:400–408. doi:10.1021/acscchembio.5b00753.
- Eyre, N. S., Johnson, S. M., Eltahla, A. A., Aloï, M., Aloia, A. L., McDevitt, C. A., ... Beard, M. R. (2017). Genome-Wide Mutagenesis of Dengue Virus Reveals Plasticity of the NS1 Protein and Enables Generation of Infectious Tagged Reporter Viruses. *Journal of virology*, 91(23), e01455-17. doi:10.1128/JVI.01455-17
- Flipse, J., Diosa-Toro, M. A., Hoornweg, T. E., van de Pol, D. P., Urcuqui-Inchima, S., & Smit, J. M. (2016). Antibody-Dependent Enhancement of Dengue Virus Infection in Primary Human Macrophages; Balancing Higher Fusion against Antiviral Responses. *Scientific reports*, 6, 29201. doi:10.1038/srep29201
- Fritz, R., Blazevic, J., Taucher, C., Pangerl, K., Heinz, F. X., & Stiasny, K. (2011). The unique transmembrane hairpin of flavivirus fusion protein E is essential for membrane fusion. *Journal of virology*, 85(9), 4377–4385. doi:10.1128/JVI.02458-10
- Gillespie, L. K., Hoenen, A., Morgan, G., & Mackenzie, J. M. (2010). The endoplasmic reticulum provides the membrane platform for biogenesis of the flavivirus replication complex. *Journal of virology*, 84(20), 10438–10447. doi:10.1128/JVI.00986-10
- Goffard, A., Callens, N., Bartosch, B., Wychowski, C., Cosset, F. L., Montpellier, C., & Dubuisson, J. (2005). Role of N-linked glycans in the functions of hepatitis C virus envelope glycoproteins. *Journal of virology*, 79(13), 8400–8409. doi:10.1128/JVI.79.13.8400-8409.2005
- Gong, Y., & Cun, W. (2019). The Role of ApoE in HCV Infection and Comorbidity. *International journal of molecular sciences*, 20(8), 2037. doi:10.3390/ijms20082037
- Gonzalez ME, Carrasco L (2003) Viroporins. *FEBS Lett* 552: 28–34.

- Gromowski, G. D., Barrett, N. D., & Barrett, A. D. (2008). Characterization of dengue virus complex-specific neutralizing epitopes on envelope protein domain III of dengue 2 virus. *Journal of virology*, 82(17), 8828–8837. doi:10.1128/JVI.00606-08
- Henry B. (2018). DRUG PRICING & CHALLENGES TO HEPATITIS C TREATMENT ACCESS. *Journal of health & biomedical law*, 14, 265–283.
- Janeway CA Jr, Travers P, Walport M, et al. Immunobiology: The Immune System in Health and Disease. 5th edition. New York: Garland Science; 2001. The interaction of the antibody molecule with specific antigen.
- Jones, C. T., Ma, L., Burgner, J. W., Groesch, T. D., Post, C. B., & Kuhn, R. J. (2003). Flavivirus capsid is a dimeric alpha-helical protein. *Journal of virology*, 77(12), 7143–7149. doi:10.1128/jvi.77.12.7143-7149.2003
- Jubin, R., Vantuno, N. E., Kieft, J. S., Murray, M. G., Doudna, J. A., Lau, J. Y., & Baroudy, B. M. (2000). Hepatitis C virus internal ribosome entry site (IRES) stem loop IIIId contains a phylogenetically conserved GGG triplet essential for translation and IRES folding. *Journal of virology*, 74(22), 10430–10437. doi:10.1128/jvi.74.22.10430-10437.2000
- Kanai, R., Kar, K., Anthony, K., Gould, L. H., Ledizet, M., Fikrig, E., ... Modis, Y. (2006). Crystal structure of west nile virus envelope glycoprotein reveals viral surface epitopes. *Journal of virology*, 80(22), 11000–11008. doi:10.1128/JVI.01735-06
- Kelley, J. F., Kaufusi, P. H., Volper, E. M., & Nerurkar, V. R. (2011). Maturation of dengue virus nonstructural protein 4B in monocytes enhances production of dengue hemorrhagic fever-associated chemokines and cytokines. *Virology*, 418(1), 27–39. doi:10.1016/j.virol.2011.07.006
- Khromykh, A. A., Sedlak, P. L., & Westaway, E. G. (2000). cis- and trans-acting elements in flavivirus RNA replication. *Journal of virology*, 74(7), 3253–3263. doi:10.1128/jvi.74.7.3253-3263.2000
- Kimple, M. E., Brill, A. L., & Pasker, R. L. (2013). Overview of affinity tags for protein purification. *Current protocols in protein science*, 73, 9.9.1–9.9.23. doi:10.1002/0471140864.ps0909s73
- Kinchen, V. J., Zahid, M. N., Flyak, A. I., Soliman, M. G., Learn, G. H., Wang, S., ... Bailey, J. R. (2018). Broadly Neutralizing Antibody Mediated Clearance of Human Hepatitis C Virus Infection. *Cell host & microbe*, 24(5), 717–730.e5. doi:10.1016/j.chom.2018.10.012
- Kong, L., Giang, E., Nieuwma, T., Kadam, R. U., Cogburn, K. E., Hua, Y., ... Law, M. (2013). Hepatitis C virus E2 envelope glycoprotein core structure. *Science (New York, N.Y.)*, 342(6162), 1090–1094. doi:10.1126/science.1243876
- Kong, L., Lee, D. E., Kadam, R. U., Liu, T., Giang, E., Nieuwma, T., Garces, F., Tzarum, N., Woods, V. L., Jr, Ward, A. B., Li, S., Wilson, I. A., & Law, M. (2016). Structural flexibility at a major conserved antibody target on hepatitis C virus E2 antigen. *Proceedings of the National Academy of Sciences of the United States of America*, 113(45), 12768–12773. <https://doi.org/10.1073/pnas.1609780113>
- Kremers, G. J., Gilbert, S. G., Cranfill, P. J., Davidson, M. W., & Piston, D. W. (2011). Fluorescent proteins at a glance. *Journal of cell science*, 124(Pt 2), 157–160. doi:10.1242/jcs.072744

- Kuhn, R. J., Dowd, K. A., Beth Post, C., & Pierson, T. C. (2015). Shake, rattle, and roll: Impact of the dynamics of flavivirus particles on their interactions with the host. *Virology*, *479-480*, 508–517. doi:10.1016/j.virol.2015.03.025
- Kuhn, R. J., Zhang, W., Rossmann, M. G., Pletnev, S. V., Corver, J., Lenches, E., ... Strauss, J. H. (2002). Structure of dengue virus: implications for flavivirus organization, maturation, and fusion. *Cell*, *108*(5), 717–725. doi:10.1016/s0092-8674(02)00660-8
- Lavie M, Goffard A, Dubuisson J. HCV Glycoproteins: Assembly of a Functional E1–E2 Heterodimer. In: Tan SL, editor. *Hepatitis C Viruses: Genomes and Molecular Biology*. Norfolk (UK): Horizon Bioscience; 2006. Chapter 4.
- Law, J., Logan, M., Wong, J., Kundu, J., Hockman, D., Landi, A., Chen, C., Crawford, K., Wininger, M., Johnson, J., Mesa Prince, C., Dudek, E., Mehta, N., Tyrrell, D. L., & Houghton, M. (2018). Role of the E2 Hypervariable Region (HVR1) in the Immunogenicity of a Recombinant Hepatitis C Virus Vaccine. *Journal of virology*, *92*(11), e02141-17. <https://doi.org/10.1128/JVI.02141-17>
- Li, L., Lok SM, Yu IM, Zhang Y, Kuhn RJ, Chen J, Rossmann MG. (2008). The flavivirus precursor membrane-envelope protein complex: structure and maturation. *Science* *319*:1830–1834. doi:10.1126/science.1153263.
- Li, T., Zhao, Q., Yang, X., Chen, C., Yang, K., Wu, C., Zhang, T., Duan, Y., Xue, X., Mi, K., Ji, X., Wang, Z., & Yang, H. (2018). Structural insight into the Zika virus capsid encapsulating the viral genome. *Cell research*, *28*(4), 497–499. <https://doi.org/10.1038/s41422-018-0007-9>
- Lindenbach, B. D., & Rice, C. M. (2013). The ins and outs of hepatitis C virus entry and assembly. *Nature reviews. Microbiology*, *11*(10), 688–700. doi:10.1038/nrmicro3098
- Ma, L., Jones, C. T., Groesch, T. D., Kuhn, R. J., & Post, C. B. (2004). Solution structure of dengue virus capsid protein reveals another fold. *Proceedings of the National Academy of Sciences of the United States of America*, *101*(10), 3414–3419. <https://doi.org/10.1073/pnas.0305892101>
- Matsui, K., Gromowski, G. D., Li, L., & Barrett, A. D. (2010). Characterization of a dengue type-specific epitope on dengue 3 virus envelope protein domain III. *The Journal of general virology*, *91*(Pt 9), 2249–2253. doi:10.1099/vir.0.021220-0
- McNabb, D. S., Reed, R., & Marciniak, R. A. (2005). Dual luciferase assay system for rapid assessment of gene expression in *Saccharomyces cerevisiae*. *Eukaryotic cell*, *4*(9), 1539–1549. doi:10.1128/EC.4.9.1539-1549.2005
- Millman, A. J., Nelson, N. P., & Vellozzi, C. (2017). Hepatitis C: Review of the Epidemiology, Clinical Care, and Continued Challenges in the Direct Acting Antiviral Era. *Current epidemiology reports*, *4*(2), 174–185. doi:10.1007/s40471-017-0108-x
- Miyazawa, Y., Atsuzawa, K., Usuda, N. *et al.* The lipid droplet is an important organelle for hepatitis C virus production. *Nat Cell Biol* **9**, 1089–1097 (2007) doi:10.1038/ncb1631

- Morales, M. A., Fabbri, C. M., Zunino, G. E., Kowalewski, M. M., Luppó, V. C., Enría, D. A., ... Calderón, G. E. (2017). Detection of the mosquito-borne flaviviruses, West Nile, Dengue, Saint Louis Encephalitis, Ilheus, Bussuquara, and Yellow Fever in free-ranging black howlers (*Alouatta caraya*) of Northeastern Argentina. *PLoS neglected tropical diseases*, *11*(2), e0005351. doi:10.1371/journal.pntd.0005351
- Mukhopadhyay S., Kim B.S., Chipman P.R., Rossmann M.G., Kuhn R.J. (2003). Structure of West Nile Virus. *Science*. Oct 10; 302(5643):248.
- Mukhopadhyay, S., Kuhn, R. & Rossmann, M. A structural perspective of the *flavivirus* life cycle. *Nat Rev Microbiol* **3**, 13–22 (2005) doi:10.1038/nrmicro1067
- Murray, C. L., Jones, C. T., & Rice, C. M. (2008). Architects of assembly: roles of Flaviviridae non-structural proteins in virion morphogenesis. *Nature reviews. Microbiology*, *6*(9), 699–708. doi:10.1038/nrmicro1928
- Neufeldt, C., Cortese, M., Acosta, E. *et al.* Rewiring cellular networks by members of the *Flaviviridae* family. *Nat Rev Microbiol* **16**, 125–142 (2018) doi:10.1038/nrmicro.2017.170
- Oliphant, T., Nybakken, G. E., Austin, S. K., Xu, Q., Bramson, J., Loeb, M., ... Diamond, M. S. (2007). Induction of epitope-specific neutralizing antibodies against West Nile virus. *Journal of virology*, *81*(21), 11828–11839. doi:10.1128/JVI.00643-07
- Patkar, C. G., & Kuhn, R. J. (2008). Yellow Fever virus NS3 plays an essential role in virus assembly independent of its known enzymatic functions. *Journal of virology*, *82*(7), 3342–3352. doi:10.1128/JVI.02447-07
- Pfaender, S., Helfritz, F. A., Siddharta, A., Todt, D., Behrendt, P., Heyden, J., ... Steinmann, E. (2018). Environmental Stability and Infectivity of Hepatitis C Virus (HCV) in Different Human Body Fluids. *Frontiers in microbiology*, *9*, 504. doi:10.3389/fmicb.2018.00504
- Prentoe, J., & Bukh, J. (2011). Hepatitis C virus expressing flag-tagged envelope protein 2 has unaltered infectivity and density, is specifically neutralized by flag antibodies and can be purified by affinity chromatography. *Virology*, *409*(2), 148–155. <https://doi.org/10.1016/j.virol.2010.10.034>
- Rajapakse S. (2011). Dengue shock. *Journal of emergencies, trauma, and shock*, *4*(1), 120–127. doi:10.4103/0974-2700.76835
- Rastogi, M., Sharma, N., & Singh, S. K. (2016). Flavivirus NS1: a multifaceted enigmatic viral protein. *Virology journal*, *13*, 131. doi:10.1186/s12985-016-0590-7
- Richardson JS. (1981). The anatomy and taxonomy of protein structure. *Adv Protein Chem* **34**:167–339. doi:10.1016/S0065-3233(08)60520-3
- Ruggli N, Rice CM. (1999). Functional cDNA clones of the Flaviviridae: strategies and applications. *Adv Virus Res* *53*:183–207. doi:10.1016/S0065-3527(08)60348-6.
- Santolini, E., Pacini, L., Fipaldini, C., Migliaccio, G., & Monica, N. (1995). The NS2 protein of hepatitis C virus is a transmembrane polypeptide. *Journal of virology*, *69*(12), 7461–7471.
- Sasaki, M. *et al.* (2018). Development of a rapid and quantitative method for the analysis of viral entry and release using a NanoLuc luciferase complementation assay. *Virus Res*. *243*, 69–74.

- Schmitt, M., Scrima, N., Radujkovic, D., Caillet-Saguy, C., Simister, P. C., Friebe, P., ... Bressanelli, S. (2011). A comprehensive structure-function comparison of hepatitis C virus strain JFH1 and J6 polymerases reveals a key residue stimulating replication in cell culture across genotypes. *Journal of virology*, 85(6), 2565–2581. doi:10.1128/JVI.02177-10
- Schwinn MK, Machleidt T, Zimmerman K, Eggers CT, Dixon AS, Hurst R, Hall MP, Encell LP, Binkowski BF, Wood KV. (2017). CRISPR-mediated tagging of endogenous proteins with a luminescent peptide. *ACS Chem Biol* doi:10.1021/acscchembio.7b00549.
- Setoh, Y. X., Tan, C. S., Prow, N. A., Hobson-Peters, J., Young, P. R., Khromykh, A. A., & Hall, R. A. (2015). The I22V and L72S substitutions in West Nile virus prM protein promote enhanced prM/E heterodimerisation and nucleocapsid incorporation. *Virology journal*, 12, 72. <https://doi.org/10.1186/s12985-015-0303-7>
- Sevvana, M., Long, F., Miller, A. S., Klose, T., Buda, G., Sun, L., Kuhn, R. J., & Rossmann, M. G. (2018). Refinement and Analysis of the Mature Zika Virus Cryo-EM Structure at 3.1 Å Resolution. *Structure (London, England: 1993)*, 26(9), 1169–1177.e3. <https://doi.org/10.1016/j.str.2018.05.006>
- Shimoike, T., Mimori, S., Tani, H., Matsuura, Y., & Miyamura, T. (1999). Interaction of hepatitis C virus core protein with viral sense RNA and suppression of its translation. *Journal of virology*, 73(12), 9718–9725.
- Shiryaev, S. A., & Strongin, A. Y. (2010). Structural and functional parameters of the flaviviral protease: a promising antiviral drug target. *Future virology*, 5(5), 593–606. doi:10.2217/fvl.10.39
- Sirohi, D., Chen, Z., Sun, L., Klose, T., Pierson, T. C., Rossmann, M. G., & Kuhn, R. J. (2016). The 3.8 Å resolution cryo-EM structure of Zika virus. *Science (New York, N.Y.)*, 352(6284), 467–470. doi:10.1126/science.aaf5316
- Stocks, C. E., & Lobigs, M. (1998). Signal peptidase cleavage at the flavivirus C-prM junction: dependence on the viral NS2B-3 protease for efficient processing requires determinants in C, the signal peptide, and prM. *Journal of virology*, 72(3), 2141–2149.
- Ströh, L. J., Nagarathinam, K., & Krey, T. (2018). Conformational Flexibility in the CD81-Binding Site of the Hepatitis C Virus Glycoprotein E2. *Frontiers in immunology*, 9, 1396. <https://doi.org/10.3389/fimmu.2018.01396>
- Sun, H., Chen, Q., & Lai, H. (2017). Development of Antibody Therapeutics against Flaviviruses. *International journal of molecular sciences*, 19(1), 54. doi:10.3390/ijms19010054
- Tamura, T., Fukuhara, T., Uchida, T., Ono, C., Mori, H., Sato, A., ... Matsuura, Y. (2018). Characterization of Recombinant Flaviviridae Viruses Possessing a Small Reporter Tag. *Journal of virology*, 92(2), e01582-17. doi:10.1128/JVI.01582-17
- Tamura, T., Igarashi, M., Enkhbold, B., Suzuki, T., Okamatsu, M., Ono, C., ... Matsuura, Y. (2019). In Vivo Dynamics of Reporter Flaviviridae Viruses. *Journal of Virology*, 93(22). <https://doi.org/10.1128/jvi.01191-19>

- Therkelsen, M. D., Klose, T., Vago, F., Jiang, W., Rossmann, M. G., & Kuhn, R. J. (2018). Flaviviruses have imperfect icosahedral symmetry. *Proceedings of the National Academy of Sciences of the United States of America*, *115*(45), 11608–11612. doi:10.1073/pnas.1809304115
- Thorn K. (2017). Genetically encoded fluorescent tags. *Molecular biology of the cell*, *28*(7), 848–857. doi:10.1091/mbc.E16-07-0504
- Vasiliauskaite, I., Owsianka, A., England, P., Khan, A. G., Cole, S., Bankwitz, D., Fong, S., Pietschmann, T., Marcotrigiano, J., Rey, F. A., Patel, A. H., & Krey, T. (2017). Conformational Flexibility in the Immunoglobulin-Like Domain of the Hepatitis C Virus Glycoprotein E2. *mBio*, *8*(3), e00382-17. <https://doi.org/10.1128/mBio.00382-17>
- Vieyres, G., Dubuisson, J., & Pietschmann, T. (2014). Incorporation of hepatitis C virus E1 and E2 glycoproteins: the keystones on a peculiar virion. *Viruses*, *6*(3), 1149–1187. doi:10.3390/v6031149
- Wen, D., Li, S., Dong, F., Zhang, Y., Lin, Y., Wang, J., ... Zheng, A. (2018). N-glycosylation of Viral E Protein Is the Determinant for Vector Midgut Invasion by Flaviviruses. *mBio*, *9*(1), e00046-18. doi:10.1128/mBio.00046-18
- World Health Organization Fact Sheet: Dengue Virus. (2019, Nov 4). Retrieved January 9, 2020, from <https://www.who.int/news-room/fact-sheets/detail/hepatitis-c>.
- World Health Organization Fact Sheet: Hepatitis C. (2019, July 9). Retrieved January 9, 2020, from <https://www.who.int/news-room/fact-sheets/detail/hepatitis-c>.
- Wozniak AL, Griffin S, Rowlands D, Harris M, Yi M, Lemon SM, et al. (2010) Intracellular Proton Conductance of the Hepatitis C Virus p7 Protein and Its Contribution to Infectious Virus Production. *PLoS Pathog* *6*(9): e1001087. <https://doi.org/10.1371/journal.ppat.1001087>
- Yasui, K., Wakita, T., Tsukiyama-Kohara, K., Funahashi, S. I., Ichikawa, M., Kajita, T., ... Kohara, M. (1998). The native form and maturation process of hepatitis C virus core protein. *Journal of virology*, *72*(7), 6048–6055.
- Yu, I. M., Holdaway, H. A., Chipman, P. R., Kuhn, R. J., Rossmann, M. G., & Chen, J. (2009). Association of the pr peptides with dengue virus at acidic pH blocks membrane fusion. *Journal of virology*, *83*(23), 12101–12107. doi:10.1128/JVI.01637-09
- Yu, K., Sheng, Z. Z., Huang, B., Ma, X., Li, Y., Yuan, X., ... Sun, H. (2013). Structural, antigenic, and evolutionary characterizations of the envelope protein of newly emerging Duck Tembusu Virus. *PloS one*, *8*(8), e71319. doi:10.1371/journal.pone.0071319
- Zhang, X., Jia, R., Shen, H., Wang, M., Yin, Z., & Cheng, A. (2017). Structures and Functions of the Envelope Glycoprotein in Flavivirus Infections. *Viruses*, *9*(11), 338. doi:10.3390/v9110338